



저작자표시-비영리-변경금지 2.0 대한민국

이용자는 아래의 조건을 따르는 경우에 한하여 자유롭게

- 이 저작물을 복제, 배포, 전송, 전시, 공연 및 방송할 수 있습니다.

다음과 같은 조건을 따라야 합니다:



저작자표시. 귀하는 원저작자를 표시하여야 합니다.



비영리. 귀하는 이 저작물을 영리 목적으로 이용할 수 없습니다.



변경금지. 귀하는 이 저작물을 개작, 변형 또는 가공할 수 없습니다.

- 귀하는, 이 저작물의 재이용이나 배포의 경우, 이 저작물에 적용된 이용허락조건을 명확하게 나타내어야 합니다.
- 저작권자로부터 별도의 허가를 받으면 이러한 조건들은 적용되지 않습니다.

저작권법에 따른 이용자의 권리는 위의 내용에 의하여 영향을 받지 않습니다.

이것은 [이용허락규약\(Legal Code\)](#)을 이해하기 쉽게 요약한 것입니다.

[Disclaimer](#)

공학석사 학위논문

Development of the Conceptual
Fire & Explosion Risk
Assessment-base model
in Pre-FEED stage

Pre-FEED 단계에서 개념적 화재 & 폭발 위험도
평가를 위한 기반 모델 개발

2017 년 08 월

서울대학교 대학원

조선해양공학과

이 경 수

Development of the Conceptual
Fire & Explosion Risk
Assessment—base model
in Pre—FEED stage

지도 교수 장 범 선

이 논문을 공학석사 학위논문으로 제출함

2017 년 8 월

서울대학교 대학원
조선해양공학과
이 경 수

이경수의 공학석사 학위논문을 인준함

2017 년 8 월

위 원 장 _____ 임 영 섭 (인)

부위원장 _____ 장 범 선 (인)

위 원 _____ 서 유 택 (인)

Abstract

Development of the Conceptual Fire & Explosion Risk Assessment–base model in Pre–FEED stage

Lee Kyeongsu

Department of Naval Architecture and Ocean
Engineering

The Graduate School

Seoul National University

The offshore platforms have a number of equipment in process area. This process area faces a high probability of hydrocarbon fire accident because most of equipment are contained the flammable oil and gas circumstances. Therefore, the fire risk

analysis is an essential safety study which should be considered in the whole development phases of an offshore platform installation. Based on the information at each development phase and level of data, the fire risk analysis results are reflected into the design with increasing the level of accuracy. However, the results of fire risk analysis considering the initial process data and layout data are conservative because most of fire risk analysis is performed under assumptions and insufficient input data in pre-FEED stage.

There is a need for a way to develop an integrated system to overcome the problems of the existing fire risk analysis method. The scope of this study is to develop the integrated system, which is required to respond with the data quickly from process design and improve FRA results in pre-FEED stage. This system is named as Integrated Fire & Explosion Conceptual Risk Analysis (IFECRA) system.

The basis of the fire risk analysis input data is defined from the process and layout information, and this study proposes the standard data transfer sheet. In addition, this study develops the modules which calculate the leak frequency automatically and generate a simplified 3D model. Therefore, the IFECRA is able to

work with 3D fire CFD simulation using a 3D simplified model. Furthermore, the fire risk analysis module develops to determine the failure of critical targets and the rate of passive fire protection based on the design accidental loads. Using the developed IFECRA system, the fire risk analysis is automatically calculated, and the design effect zone is obtained from the both CFD model and analytical model fire simulation results. Quantitative comparison between the failure of critical targets and the rate of passive fire protection are done by employing the design effect zone.

For results of the fire risk analysis, it is confirmed that the risk analysis results using the IFECRA system have relatively accurate compared to the existing fire risk analysis method.

Keywords : Quantitative risk assessment, Fire risk analysis, Offshore, Topside, Process area, Integrated system, Computational fluid dynamics, Analytical model

Student Number : 2015–21169

Contents

1.	Introduction	13
1.1.	Research Background	13
1.2.	State of Art	14
1.2.1.	Flame–Size–Based Approach	15
1.2.2.	Heat–Dose–Based Approach	16
1.2.3.	Exceedance–Curve–Based Approach.....	17
1.2.4.	Cumulative Failure Frequency–Based Approach.....	17
1.3.	Objective in This Study	18
2.	General Procedures of Fire Risk Analysis Case in Pre–FEED Stage	21
2.1.	Fire Risk Analysis Input Data	21
2.2.	Fire Scenario Identification.....	22
2.3.	Leak Frequency Calculation.....	24
2.4.	Fire Frequency Calculation	28
2.5.	Fire Simulation.....	29
2.6.	Risk Analysis	30
2.6.1.	Design Accidental Load	31
2.6.2.	Effect Zone.....	31
2.6.3.	Design Effect Zone.....	33
2.7.	Risk Control.....	35
3.	Development of Integrated Fire & Explosion Conceptual Risk Assessment System.....	38
3.1.	Introduction of IFECRA System	38
3.2.	FRA Input Data	40
3.3.	Central Database of IFECRA System.....	44

3.3.1.	Routing Algorithm: Rectilinear Method.....	48
3.3.2.	Routing Algorithm: A* Method.....	51
3.3.3.	Valve Positioning	60
3.4.	Inventory Calculation Module.....	63
3.5.	Leak Frequency Calculation Module	65
3.6.	Simplified 3D Generation Module	69
3.7.	Fire Risk Analysis Module.....	72
3.8.	User Interface.....	76
4.	Case Study.....	78
4.1.	Fire Scenario Identification	78
4.1.1.	Effective Leak Directions	82
4.2.	Leak Frequency Calculation	83
4.3.	Fire Frequency Calculation	85
4.4.	Fire Simulation.....	86
4.4.1.	Radiation Calculation	86
4.4.2.	Fire Simulation Result.....	91
4.5.	Risk Analysis	94
4.5.1.	Design Criterion.....	94
4.5.2.	Design Effect Zone.....	96
4.5.3.	Design Effect Zone Comparison	99
4.5.4.	Impact Analysis Results	102
4.6.	Risk Control.....	110
4.6.1.	Passive Fire Protection Rating Results.....	110
5.	Conclusion	114
5.1.	Summary.....	114
5.2.	Findings	115
6.	References.....	117
7.	Appendix	120

7.1.	Appendix A: Example Rule Set of Process Piping Lengths	120
7.2.	Appendix B: Constraint Conditions in Piping Algorithm	122
7.3.	Appendix C: A Simple Example of A* Algorithm ...	127

List of Figures

FIG. 1 DEVELOPMENT PHASES OF AN OFFSHORE PLATFORM INSTALLATION (TOTAL 2008)	13
FIG. 2 DIFFERENT LEVEL OF FRA STUDIES FOR EACH DEVELOPMENT PHASE.....	15
FIG. 3 GENERAL PROCEDURES OF FRA CASE.....	20
FIG. 4 FRA INPUT DATA.....	22
FIG. 5 CASE EXAMPLE OF PROCESS DESIGN WITH ISOLATABLE SEGMENTS.....	23
FIG. 6 EXAMPLE OF THE EXCEEDANCE CURVE AND DETERMINING A DESIGN ACCIDENTAL LOAD (DAL)	31
FIG. 7 EXAMPLE OF THE EFFECT ZONE BY USING ANALYTICAL MODEL (E.G. PHAST)	33
FIG. 8 (A) EXAMPLE OF EXCEEDANCE CURVE AND (B) EXAMPLE OF DESIGN EFFECT ZONE BY USING A DAL	34
FIG. 9 EXAMPLE OF FPSO PROCESS AREA LAYOUT.....	36
FIG. 10 APPLIED FRA IN IFECRA SYSTEM	39
FIG. 11 IFECRA SYSTEM FLOW DIAGRAM.....	39
FIG. 12 GENERAL OUTLINE OF DATA INTERFACE BETWEEN PROCESS SIMULATOR AND IFECRA SYSTEM.....	41
FIG. 13 CASE EXAMPLE OF DATA TRANSFER SHEET.....	42
FIG. 14 CENTRAL DATABASE OF IFECRA SYSTEM EXPRESSED BY USING CLASS DIAGRAM	47
FIG. 15 SYSTEMATIC DESCRIPTION OF END-TAG INFORMATION WITH SEARCHED EQUIPMENT INFORMATION.....	48
FIG. 16 ROUTING ALGORITHM BY USING RECTILINEAR METHOD	49
FIG. 17 EXAMPLE OF THE GENERATED SIX NODES DEPENDING ON CONNECTION CONSTRAINT CONDITION.....	50
FIG. 18 SIMPLE EXAMPLE OF ROUTING ALGORITHM BY USING RECTILINEAR METHOD.....	51
FIG. 19 ROUTING ALGORITHM BY USING A* METHOD	54
FIG. 20 EXAMPLE OF GENERATED 9 X 9 X 9 NODES IN THREE DIMENSIONAL BETWEEN EQUIPMENT (I) AND EQUIPMENT (J) ..	56

FIG. 21 EXAMPLE OF IDENTIFYING THE PRESENCE OF OBSTACLES IN 729 NODES USING THE QUANTIFIED DIMENSION OF EQUIPMENT (K)	57
FIG. 22 PRESENTATION OF THE SELECTED PATH DIRECTIONS	58
FIG. 23 ILLUSTRATION OF BENDING CONSTRAINT	59
FIG. 24 SIMPLE EXAMPLE OF ROUTING ALGORITHM BY USING A* METHOD	60
FIG. 25 CASE EXAMPLES OF PROCESS DESIGN (A) PFD/P&ID, AND (B) PROCESS SIMULATOR (E.G. HYSYS)	61
FIG. 26 EXAMPLE OF CALCULATING THE VALVE POSITION.....	62
FIG. 27 LEAK FREQUENCY CALCULATION FLOWCHART	66
FIG. 28 EXAMPLE OF THE LEAK FREQUENCY CALCULATION AT THE BLOCK BOUNDARY	68
FIG. 29 SYSTEMATIC DESCRIPTION OF THE DEVELOPED A 3D MODEL GENERATION MODULE.....	72
FIG. 30 GENERAL PROCEDURES OF THE FIRE RISK ANALYSIS MODULE	73
FIG. 31 EXAMPLE OF CALCULATING THE EXPOSURE RATE.....	75
FIG. 32 SCREENSHOT OF THE IFECRA SYSTEM.....	77
FIG. 33 FPSO PROCESS AREA IN CASE STUDY	79
FIG. 34 TIME DEPENDENT LEAK PROFILE	80
FIG. 35 SELECTED LEAK DIRECTIONS	81
FIG. 36 FIRE SIMULATION RESULT COMPARISONS THROUGH THE NUMBER OF LEAK DIRECTIONS.....	83
FIG. 37 LEAK FREQUENCY CALCULATION RESULTS BY USING DEVELOPED LEAK FREQUENCY CALCULATION MODULE	84
FIG. 38 RADIATION FLUX CALCULATED IN ONE GRID POINT [13] ...	87
FIG. 39 RADIATION INTENSITY (RAY) AND SOLID ANGLE	88
FIG. 40 VISUALIZED THE BULLET MONITOR WITH THE CALCULATED RADIATION INTENSITY (KFX 2010)	89
FIG. 41 BULLET MONITOR POINTS TO OBTAIN THE RADIATIVE HEAT FLUX AROUND FPSO TOPSIDE PROCESS AREA	91
FIG. 42 RADIATION HEAT FLUX CONTOUR COMPARISON BETWEEN (A) ANALYTICAL MODEL (PHAST) AND (B) CFD MODEL (KFX)	92
FIG. 43 JET FIRE FLAME INTERACTION WITH SURROUNDING EQUIPMENT IN CFD FIRE SIMULATION.....	93
FIG. 44 RADIATION HEAT FLUX CONTOUR COMPARISON BOTH ANALYTICAL MODEL AND CFD MODEL WITHOUT GEOMETRY	94

FIG. 45 EXAMPLE PROCEDURES OF DETERMINING THE DESIGN EFFECT ZONE BY USING RADIATION HEAT FLUX DATA FROM MONITORING POINTS.....	97
FIG. 46 DESIGN RADIATION CONTOUR AND EFFECT ZONE AT 5 MINUTES	98
FIG. 47 DESIGN RADIATION CONTOUR AND EFFECT ZONE AT 10 MINUTES	98
FIG. 48 DESIGN RADIATION CONTOUR AND EFFECT ZONE AT 30 MINUTES	98
FIG. 49 DESIGN RADIATION CONTOUR AND EFFECT ZONE AT 60 MINUTES	99
FIG. 50 DESIGN RADIATION CONTOUR AND EFFECT ZONE AT 120 MINUTES	99
FIG. 51 DESIGN EFFECT ZONES AT 5 MINUTES BETWEEN KFX AND PHAST	100
FIG. 52 DESIGN EFFECT ZONES AT 10 MINUTES BETWEEN KFX AND PHAST	101
FIG. 53 DESIGN EFFECT ZONES AT 30 MINUTES BETWEEN KFX AND PHAST	101
FIG. 54 DESIGN EFFECT ZONES AT 60 MINUTES BETWEEN KFX AND PHAST	101
FIG. 55 DESIGN EFFECT ZONES AT 120 MINUTES BETWEEN KFX AND PHAST	102
FIG. 56 THE IMPACT ANALYSIS RESULTS BY USING THE FIRE RISK ANALYSIS OF DEVELOPED IFECRA SYSTEM.....	103
FIG. 57 IMPACT ANALYSIS COMPARISON BETWEEN KFX AND PHAST (A) DESIGN EFFECT ZONE WITH CRITICAL TARGET AT 5 MINUTES (B) DESIGN EFFECT ZONE WITH CRITICAL TARGET AT 10 MINUTES	104
FIG. 58 PFP RATING RESULTS BY USING IFECRA SYSTEM	111
FIG. 59 RULE SET OF PROCESS PIPING LENGTHS.....	121
FIG. 60 VISUAL DESCRIPTIONS OF (A) THE COST OF THE PATH FROM THE START NODE TO N AND (B) THE SHORTEST PATH COST FROM NODE N TO THE END NODE	128
FIG. 61 PATH DIRECTIONS FROM NODE N	129

List of Tables

TABLE 1 CASE EXAMPLE OF LEAK FREQUENCY CALCULATION BY USING PART COUNT METHOD BASED ON ISOLATABLE SEGMENT GIVEN IN FIG. 5.....	27
TABLE 2 AN EXAMPLE OF FIRE FREQUENCY CALCULATION BASED ON ISOLATABLE SEGMENT GIVEN IN FIG. 5	29
TABLE 3 FAILURE TIME OF CRITICAL TARGET A AND DISTANCE FROM LEAK LOCATION TO CRITICAL TARGET A	35
TABLE 4 DESIGN DISTANCE FOR EACH TIME DURATION.....	36
TABLE 5 EXAMPLE OF EQUIPMENT DATA TRANSFER SHEET	43
TABLE 6 EXAMPLE OF VALVE DATA TRANSFER SHEET.....	43
TABLE 7 EXAMPLE OF PIPE DATA TRANSFER SHEET	44
TABLE 8 PROPERTIES OF THE EQUIPMENT CLASS	45
TABLE 9 PROPERTIES OF THE VALVE CLASS	45
TABLE 10 PROPERTIES OF THE PIPE CLASS.....	46
TABLE 11 KFX GEOMETRY COMMANDS (KFX 2010)	70
TABLE 12 EXAMPLE FORMAT OF KFX MODEL BASED ON FIG. 29...	71
TABLE 13 PARAMETERS FOR SCENARIO IDENTIFICATION	79
TABLE 14 LEAK FREQUENCY CALCULATION RESULTS DEPENDENT ON LEAK HOLE SIZE.....	84
TABLE 15 RESULTS OF IGNITION PROBABILITY CALCULATION BY USING COX ET AL. (1990)	85
TABLE 16 FIRE FREQUENCY CALCULATION RESULTS	85
TABLE 17 PROPERTIES OF BULLET MONITOR SETTING IN KFX.....	90
TABLE 18 DESIGN CRITERION FOR EACH CRITICAL TARGET WITH FAILURE TIME.....	95
TABLE 19 IMPACT ANALYSIS RESULT COMPARISONS IN MODULE P5	105
TABLE 20 IMPACT ANALYSIS RESULT COMPARISONS IN MODULE P6	106
TABLE 21 IMPACT ANALYSIS RESULT COMPARISONS IN MODULE S5	108
TABLE 22 RESULTS OF PFP RATING BY USING CFD MODEL (E.G. KFX).....	111
TABLE 23 RESULTS OF PFP RATING BY USING ANALYTICAL MODEL (E.G. PHAST)	112

TABLE 24 CONSTRAINT CONDITION 1.....	122
TABLE 25 CONSTRAINT CONDITION 2.....	123
TABLE 26 CONSTRAINT CONDITION 3.....	123
TABLE 27 CONSTRAINT CONDITION 4.....	124
TABLE 28 CONSTRAINT CONDITION 5.....	124
TABLE 29 CONSTRAINT CONDITION 6.....	125
TABLE 30 CONSTRAINT CONDITION 7.....	125
TABLE 31 CONSTRAINT CONDITION 8.....	126
TABLE 32 SIMPLE EXAMPLE OF PATH SEARCHING	129

NOMENCLATURE

CFD	Computational Fluid Dynamic
DAL	Design Accidental Load
DNV	Det Norske Veritas
ESD	Emergency Shutdown
ESDV	Emergency Shutdown Valve
EDP	Emergency Depressurization
FPSO	Floating Production Storage Offloading
FRA	Fire Risk Analysis
FEED	Front End Engineering Design
HC	Hydrocarbon
HSE	Health and Safety Executive
HCRD	Hydrocarbon Release Database
IFECRA	Integrated Fire & Explosion Conceptual Risk Assessment system
KFX	Kameleon FireEx
OGP	Oil & Gas Producer
PFP	Passive Fire Protection
PFD	Process Flow Diagram
Phast	Process Hazard Analysis Tool
P&ID	Ping & Instrument Diagram
QRA	Quantitative Risk Assessment
SDV	Shutdown Valve

1. Introduction

1.1. Research Background

Increasing energy consumptions, the resource exploitations expand to the sea floor in which the crude oil and gas buried. Most of the offshore platforms have a number of equipment in process area. This process area faces a high probability of hydrocarbon fire accident because most of equipment are contained the flammable oil and gas circumstance. Therefore, Fire Risk Analysis (FRA) is an essential safety study which should be considered in the whole development phases of an offshore platform installation as shown in Fig. 1.



Fig. 1 Development phases of an offshore platform installation

(Total 2008)

Most of oil major and engineering companies, they are concentrated on safety designs as reflecting FRA results from pre-

FEED stage to end of offshore development. FRA is needed a number of input data from the process design. At different development phases, different levels of FRA input data are provided from the process data and layout data. However, FRA input data are frequently changed and insufficient because process design is under development in pre-FEED stage. For these reasons, FRA is performed under assumptions and insufficient input data in pre-FEED stage.

Therefore, there is a need for a way to response frequently changed data and to improve the assumed FRA in pre-FEED stage. The development of integrated system is needed to response data quickly from process design and improve FRA results in pre-FEED stage. The system is called the Integrated Fire & Explosion Conceptual Risk Assessment (IFECRA) system.

1.2. State of Art

There have been many studies on FRA at different development phase of an offshore installation as shown in Fig. 2. In this chapter, three representative FRA studies are briefly explained. First one is the method of “flame-size-based approach” proposed

by Krueger & Smith (2003), which is usually adopted in pre-FEED/FEED stage. The second method is “heat-dose-based approach” published in FABIG (2009) and third one is “cumulative failure frequency-based approach” proposed by Jin & Jang (2015). Both of second and third methods are usually applied in detailed engineering development phase. The details of each method is briefly introduced in the following sections. Detailed descriptions are briefly summarized as follows.

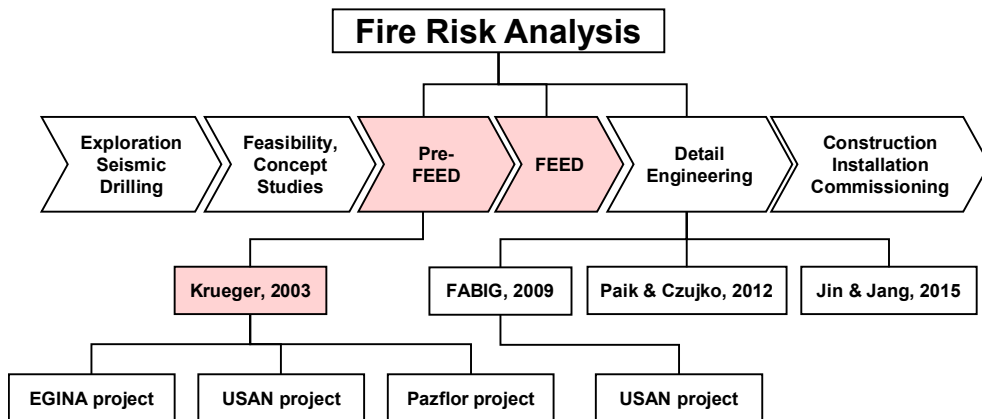


Fig. 2 Different level of FRA studies for each development phase

1.2.1.Flame-Size-Based Approach

In pre-FEED/FEED stage of an offshore platform installation, FRA concentrates on possible consequences associated with potential fire scenarios in terms of impact analysis and PFP application under critical targets. The representative method is the flame-size-based approach (Krueger and Smith, 2003). It evaluates the failure of critical targets or process modules using a design flame size obtained from fire simulation. In pre-FEED stage, however, a 3D geometric model is not available because the process data and the layout data are under development. Hence, fire simulation is usually performed using an analytical model without a 3D geometric information. This analytical model provides a conservative fire simulation results, therefore overall FRA results are conservative too. The flame size-based approach is not adequate for detail engineering stage for detail structural consequence analysis.

1.2.2.Heat-Dose-Based Approach

FABIG (2009) proposes a heat-dose-based approach which is probabilistically assessed the fire load and structural response by adopting a conventional exceedance curve of heat dose. Notes that

a heat dose is defined as the time integral of radiation heat flux. In detailed engineering stage, a 3D geometric model is used because the process data and the layout data are fully available. Hence, the 3D CFD model can be implemented in FRA. Therefore, overall FRA results are obtained accurately through fire simulation used CFD model than analytical model.

1.2.3.Exceedance–Curve–Based Approach

Paik et.al (2011) and Paik and Czujko (2012) proposed the EFEF JIP (explosion and fire engineering of FPSO units) method in detailed engineering stage. The EFEF JIP randomly generates fire scenarios by input of several random variables associated with individual probability density functions. Using the method, a fire load can be assessed probabilistically by employing an exceedance curve. In this time, the consequence modelling adopts a 3D CFD model because a 3D geometric mode is available.

1.2.4.Cumulative Failure Frequency–Based Approach

Jin and Jang (2015) proposes a cumulative failure frequency–based approach where the failure of each structural member is judged by probabilistically assessing the cumulative failure frequency (CFF) of each member in detailed engineering stage. This procedure is to identify the critical structure member that has a failure frequency exceeding a certain risk acceptance criterion. In this design stage, the process data and the layout data are fully available, therefore FRA usually adopts a CFD fire simulation.

1.3. Objective in This Study

Fig. 3 shows a general procedure of FRA method used in pre–FEED stage. Practical details associated with the methodologies in general procedures of FRA case will be explained following chapter.

Most of FRA input data are manually determined based on the process design (e.g PFD, P&ID). In pre–FEED stage, the process design is under development, therefore, FRA input data are frequently changed and insufficient. After the fire scenarios are finished to identify, the leak frequency should be calculated based on the identified fire scenarios. For that, the number of equipment belonged to each isolated segment is manually counted from the

process design. In addition, process design does not provide a specific piping length, hence, piping lengths are roughly estimated. For these reasons, the leak frequency calculation obtains a large variance in calculation results. Furthermore, lack of layout information and process data, FRA is not possible to use a 3D CFD fire simulation because a 3D geometric model is not available in pre-FEED stage.

Therefore, this study mainly develops an IFECRA system to respond quickly from process design and to improve overall FRA results. First of all, this study develops an IFECRA system to interface with process simulator for FRA in pre-FEED stage. Also, the piping lengths are estimated by using a routing algorithm for an accurate calculation of leak frequency. In addition, a fire simulation can be performed using CFD model based on the simplified 3D model. Finally, IFECRA system is able to automate many calculations which are required in FRA.

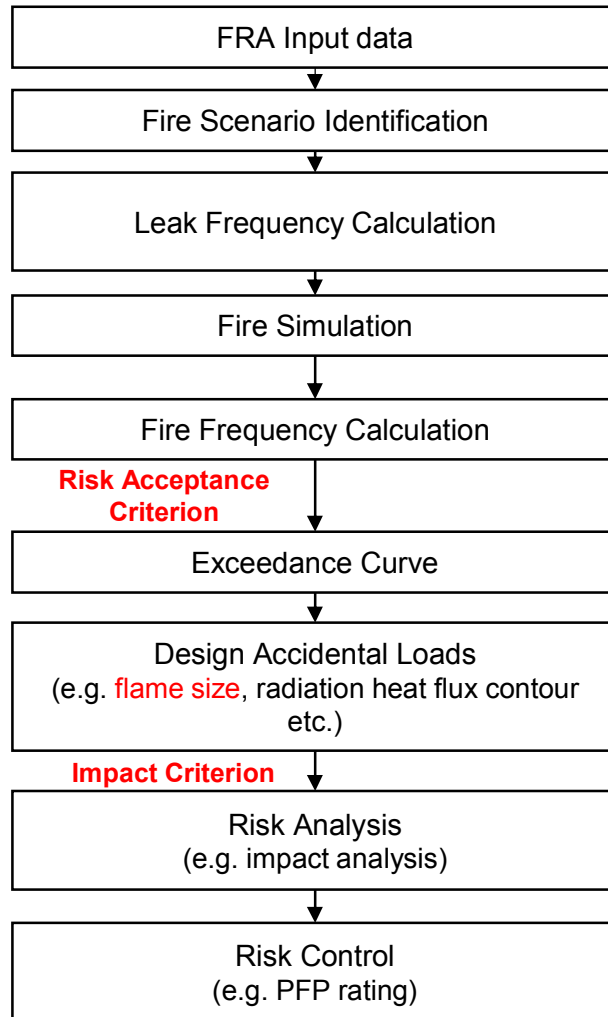


Fig. 3 General procedures of FRA case

2. General Procedures of Fire Risk Analysis

Case in Pre-FEED Stage

Fire risk analysis (FRA) is a subpart of Quantitative risk assessment (QRA) which mainly evaluates the fire risk in offshore platform. This chapter explains the general procedures (Fig. 3) of fire risk analysis case in pre-FEED stage in details.

2.1. Fire Risk Analysis Input Data

FRA input data can be categorized into process design and layout design as given in Fig. 4. In the process design, FRA input data can be divided into 3 sub-categories such as “equipment”, “inventory” and “operating conditions”. First of all, the “equipment” category can comprise different types of equipment such as pressure vessel, pipe, valve, compressor and pump. In addition, the “inventory” category includes 2 variables, namely, composition and volume. Lastly, the “operating conditions” includes the pressure and temperature. In the layout data, FRA input data includes locations of

module and equipment. These FRA input data are used in fire scenario identification.

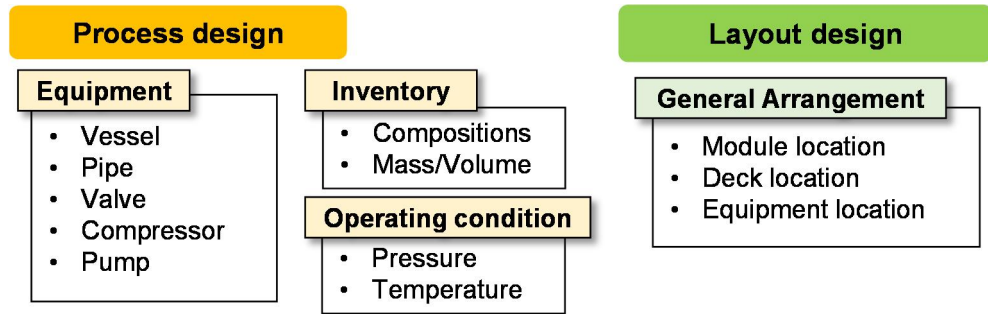


Fig. 4 FRA input data

In this study, a central database which stores FRA input data is proposed. Details of the IFECRA database are explained in chapter 3.

2.2. Fire Scenario Identification

A number of parameters are considered during the fire scenario identification such as leak rate, leak duration, leak direction, leak location, leak frequency, ignition probability and environmental variables. Among the parameters, leak rate, leak duration, leak frequency and ignition probability are predictable

because they are dependent on the process data. However, the leak location and direction are probabilistically determined due to the randomness. In order to identify the fire scenario, the whole process design can be divided into several isolatable segments (Total, 2008), and each segment is bounded by shutdown valves (SDVs) or emergency shutdown valves (ESDV). The offshore process area can be divided by several number of modules and each module is isolated by SDVs or ESDVs in accordance with standard classification (Total, 2008). Therefore, each module of offshore platform can be represented as a combination of a few isolatable segments.

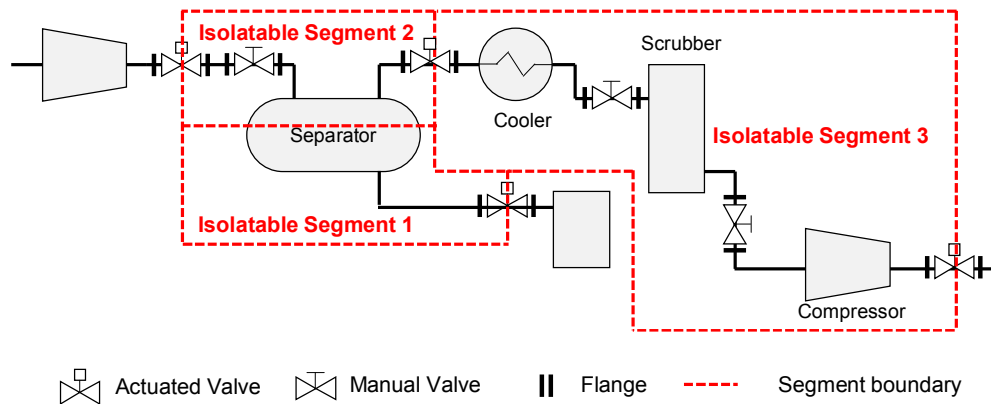


Fig. 5 Case example of process design with isolatable segments

2.3. Leak Frequency Calculation

The leak frequency of isolatable segment is usually calculated using Part Count method proposed by DNV (2011). The frequency of hydrocarbon leaks is an input to FRA study. The part count method is to count the number of equipment containing the hydrocarbon from process design. Here, the equipment includes all kinds of potential leak sources such as pressure vessel, valve, flange, piping and so on. The part count method can be defined as follows.

$$F_{leak} = \sum_{i=1}^n f_k \times N_k$$

F_{leak}	= Total frequency of identified isolatable segment
n	= The number of equipment types (e.g. pressure vessel, compressor, pump, valve and so on)
f_k	= Historical leak frequency of kth kind of equipment
N_k	= The number of kth kind of equipment in a isolatable segment

The following general rules can be applied in conducting the equipment count.

- For valves at the boundary of the isolatable segment boundary, one valve and one flange are included.
- Include the process lines containing hydrocarbon/flammable chemicals.
- If an isolatable segment contains large quantities of liquid and gas (e.g. a separator), it is assumed that 50% of the leak frequency is from the gaseous phase and 50% from the liquid phase. It is often called hierarchy principle proposed by Total (2008) [6].
- Detailed process piping arrangement is not available in pre-FEED stage. Hence, process piping lengths are roughly estimated as presented in Appendix 7.1.

In this study, historical leak database, an open source released from the Oil & Gas Production (OGP) is referred (OGP, 2010). Case example of the leak frequency can be calculated for each isolatable segment based on Fig. 5. The results of frequency calculation are listed in Table 1.

The IFECRA system is able to automate the calculation of the leak frequency. In addition, the process piping lengths can be estimated by physically arranging the pipes using a routing algorithm. Hence, the system intends to increase the accuracy and efficiency for the leak frequency calculation using the automation compared with conventional leak frequency calculation in manual way. Detailed descriptions of the leak frequency calculation in IFECRA system is laid in Chapter 3.

Table 1 Case example of leak frequency calculation by using part count method based on isolatable segment given in Fig. 5

Segment ID	Equipment Type	Quantity of equipment	Diameter	Leak frequency [6" hole diameter]	Total frequency
1	Pressure vessel	0.5	N/A*	1.70E-04	8.50E-05
1	Actuated valve	0.5	6"	6.20E-04	3.10E-04
1	Flange	1	6"	1.10E-04	1.10E-04
1	Pipe	40.5	6"	7.40E-05	3.00E-03
Total leak frequency of an isolatable segment 1					3.51E-03
2	Pressure vessel	0.5	N/A*	1.70E-04	8.50E-05
2	Actuated valve	1	6"	6.20E-04	6.20E-04
2	Manual valve	1	6"	1.30E-04	1.30E-04
2	Flange	4	6"	1.10E-04	4.40E-04
2	Pipe	40.5	6"	7.40E-05	3.00E-03
Total leak frequency of an isolatable segment 2					4.28E-03
3	Heat exchanger	1	N/A*	1.20E-04	1.20E-04
3	Pressure vessel	1	N/A*	1.70E-04	1.70E-04
3	Compressor	1	N/A*	1.10E-04	1.10E-04
3	Actuated valve	1	6"	6.20E-04	6.20E-04
3	Manual valve	2	6"	1.30E-04	2.60E-04
3	Flange	6	6"	1.10E-04	6.60E-04
3	Pipe	106.5	6"	7.40E-05	7.88E-03
Total leak frequency of an isolatable segment 3					9.82E-03

* Not applicable

2.4. Fire Frequency Calculation

The fire frequency of each identified fire scenario is calculated from the leak and several probabilities such as ignition probability and activation probability of ESD & EDP. The activation probability of ESD & EDP can be referred from Total (2008). In this study, fire frequency is calculated by multiplying the leak frequency to ignition probability. The general formulations are used for fire frequency calculation as follows.

$$F_{fire,i} = F_{leak} \times P_{ign}$$

$F_{fire,i}$	= Fire frequency of identified fire scenario i
F_{leak}	= Total frequency of identified isolatable segment
P_{ign}	= Ignition probability

The ignition probability used in this study is proposed by Cox et al. (1990). This ignition probability model is dependent on leak rate, and ignition probability equation is defined below.

$$P_{ign} = 0.0158 \times R^{0.6415}$$

P_{ign} = Ignition probability

R = Leak rate [kg/s]

An example of the fire frequency calculation for each isolatable segment of Fig. 5 is given in Table 2.

Table 2 An example of fire frequency calculation based on
isolatable segment given in Fig. 5

Segment number	Leak hole size	Total leak frequency	Ignition probability	Fire frequency
1	Large [65mm]	3.51E-03	5.75E-02	2.02E-04
2	Large [65mm]	4.28E-03	5.75E-02	2.45E-04
3	Large [65mm]	9.82E-03	5.75E-02	5.65E-04

2.5. Fire Simulation

FRA indicates that fire simulation results can be measured by the impact of critical targets by quantifying physical parameters based on fire scenarios. Typical quantified parameters are

respectively flame size and radiation heat flux contour in pre-FEED stage.

In most of pre-FEED stages, a 3D geometric model is not available due to lack of equipment layout information. Hence, the analytical model (e.g. Phast) is commonly used in this stage. However, the analytical model gives the conservative results of fire simulation because geometric information is not reflected in the fire simulation, and consequently leads to conservative risk analysis. Therefore, the IFECRA system mainly intends to use a CFD model applying a simplified 3D model to increase the accuracy of fire simulation result. Detailed description of the 3D generation module of IFECRA system is explained in Chapter 3.

2.6. Risk Analysis

Fire risk analysis is performed by applying fire consequences with corresponding fire frequencies based on identified fire scenarios. In this section, the impacts (i.e. failure of critical targets) can be determined using the design accidental loads (DALs).

2.6.1.Design Accidental Load

The design accidental load (DAL) is determined employing the exceedance curve which is generated using fire consequences and fire frequencies. The risk acceptance criterion (i.e. 10^{-4}) is used to select the DAL for fire load (NORSOK 2001). Fig. 6 presents an example of the exceedance curve and determining a DAL for the risk acceptance criteria.

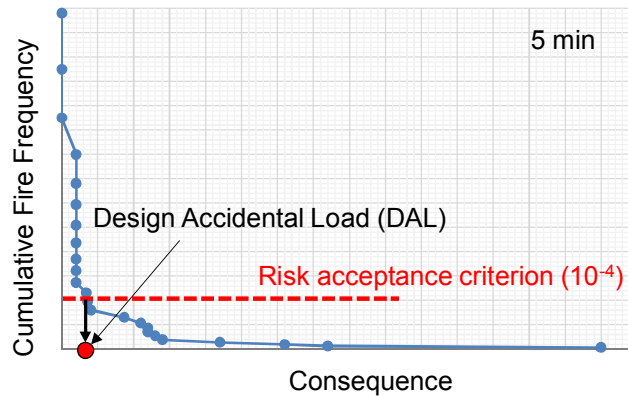


Fig. 6 Example of the exceedance curve and determining a design accidental load (DAL)

2.6.2.Effect Zone

The failure of critical target is judged by the fire simulation results. The analytical model (e.g. Phast) can provide flame size and distance from leak location to specific radiation level. The effect zone used in the analytical model can be drawn with a circle using the flame size or a contour of specific radiation level. Fig. 7 presents an example of the effect zone defined by a contour of specific radiation level.

However, in CFD model, it is not possible to draw a circle because the flame size is not calculated in CFD model (e.g. Kameleon FireEx, KFX). Instead, the radiation heat flux contour is used to judge the failure of critical targets. Detailed explanation of the effect zone is provided in Chapter 4.

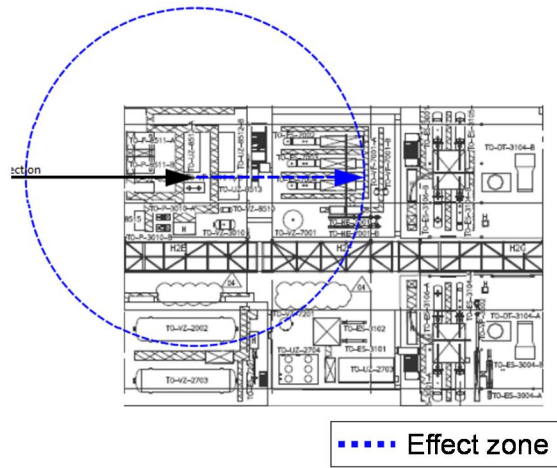
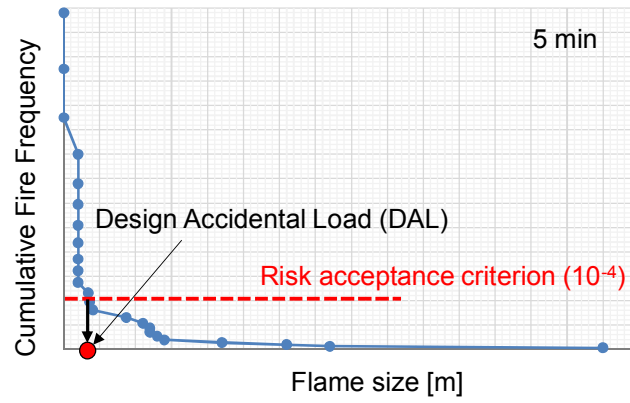


Fig. 7 Example of the effect zone by using analytical model (e.g. Phast)

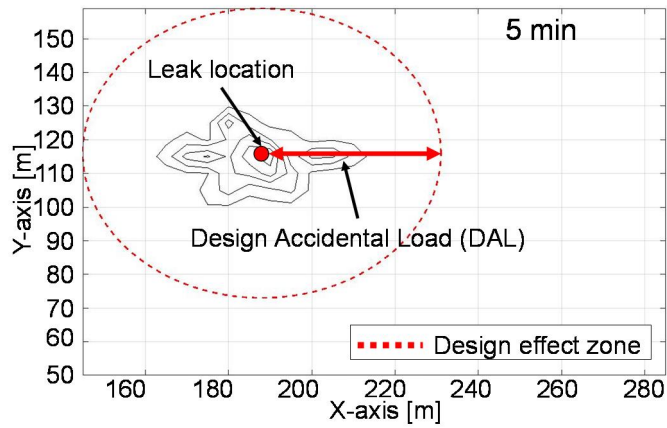
2.6.3.Design Effect Zone

The design effect zone, a contour circle of the design accidental load at each time interval, is used for judging the failure of critical targets by checking whether to locate inside the circle or not.

Again, the design effect zone can be represented by a circle measuring the design flame size or a contour of specific radiation level. Fig. 8 (b) presents an example of the design effect zone using design accidental load determining from Fig. 8 (a).



(a)



(b)

Fig. 8 (a) Example of exceedance curve and (b) Example of design effect zone by using a DAL

2.7. Risk Control

The design effect zone provides a criterion of the failure of critical target. The judgement is enabled by whether a critical target locates inside in a design circular contour of specific radiation level or not. Fig. 9 shows an example module layout of FPSO process area, and design distance from leak location to specific radiation level is determined as listed in Table 4. Table 3 shows the failure time of critical target A. The critical target A becomes failed when it is continuously exposed to fire accident. The distance between A and leak location is 9m and design criterion (i.e. failure time) is 5 min. During the first 5 min, the distance is bigger than the magnitude of design distance. It indicates that the critical target A fails if it is not provided any fire protection.

Table 3 Failure time of critical target A and distance from leak location to critical target A

Critical target: A	
Time to failure (min)	5
Distance from leak location to specific radiation level (m) at 5 min after leak	13

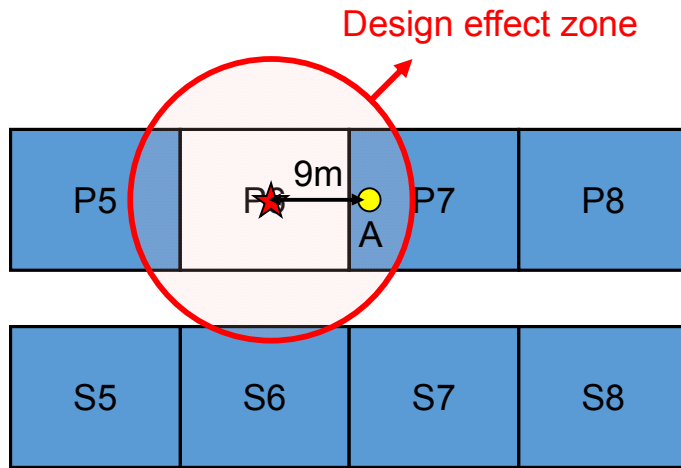


Fig. 9 Example of FPSO process area layout

Table 4 Design distance for each time duration

Design distance from leak location to specific radiation level at each moment					
Time (min)	5	10	30	60	120
Distance (m)	13	11	10	8.5	7.5

Therefore, critical target A needs the rate of Passive Fire Protection (PFP). Other design distances at each time given in Table 4 is utilized to determine the PFP rating. In example, the design distance is kept bigger than the distance between critical target A and leak location before 60 min. It concludes that the minimum rate of PFP for critical target A should be J30.

The IFECRA system proposed in this study, the failure of critical targets and the determination of the rate of FPF is automated. Detailed descriptions of the determination of failed critical target and the rate of PFP in the IFECRA system are demonstrated in Chapter 3.

3. Development of Integrated Fire & Explosion Conceptual Risk Assessment System

3.1. Introduction of IFECRA System

The development of an integrated system called IFECRA system is based on FRA methodology in pre-FEED stage, and applied FRA in the IFECRA system is described in Fig. 10. Central database of IFECRA system can collect FRA input data which automatically transferred from process simulator and layout data. It seems that the IFECRA system increases the efficiency through interface with process simulator (e.g. HYSYS). FRA input data and data interface are described in the following sections.

Fig. 11 presents a general outline of the developed IFECRA system with relevant modules such as inventory calculation module, leak frequency calculation module, 3D model generation module and fire risk analysis module.

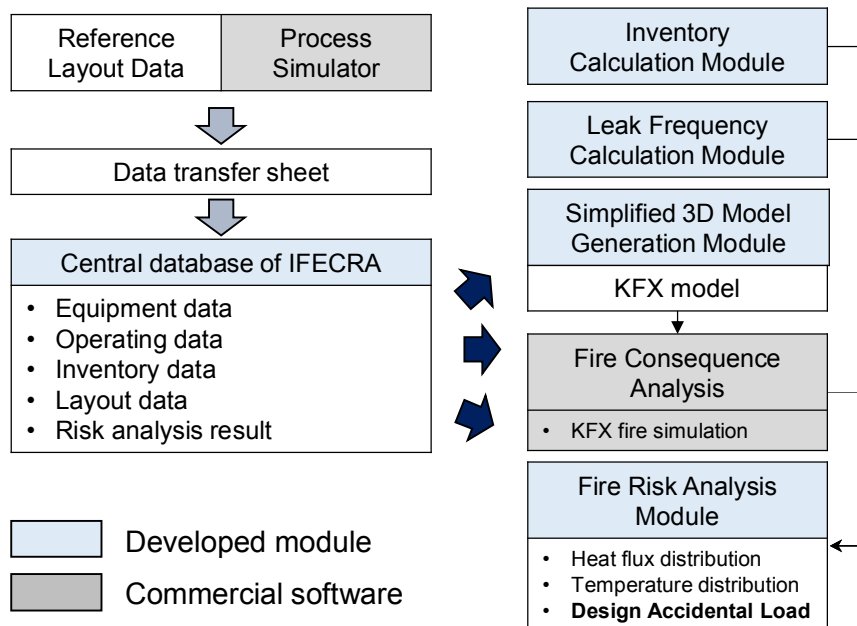


Fig. 10 Applied FRA in IFECA system

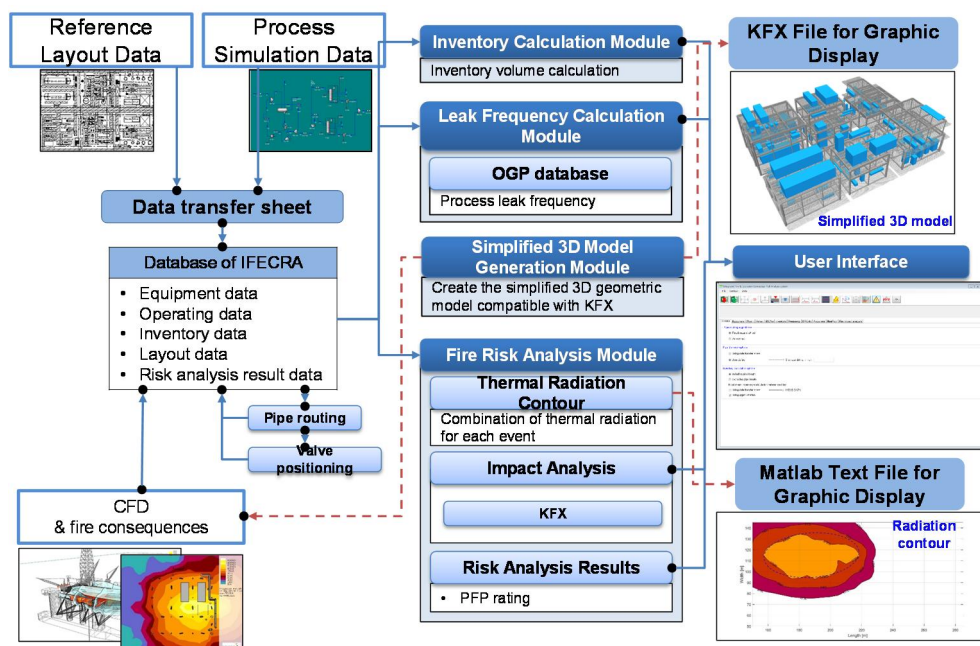


Fig. 11 IFECA system flow diagram

After consequence modelling, design accidental load (DAL) can be determined through the fire simulation result and fire frequency. Importing the design accidental load (DAL) into the system, the system is available to analyze the failure of critical targets automatically which are exposed under fire loads. Finally, the Passive Fire Protection (PFP) rating can be determined based on failure of critical targets. All these results can be found in user interface of the developed IFECRA system. Detailed descriptions of the developed modules are explained as follows

3.2. FRA Input Data

FRA input data has investigated referring the existing FRA methodology in pre-FEED stage. FRA input data can be defined in terms of process through interface with process simulator. In addition, FRA input data can be defined in terms of layout by employing the reference layout data. This study proposes a ‘standard data transfer sheet’ which contains FRA input data from process simulator and reference ship layout. Overall interface procedure is described in Fig. 12. FRA input data in terms of process design can be extracted from process simulator (e.g.

HYSYS) by proposed standard data transfer sheet. The IFECRA system imports the extracted data of standard data transfer sheet.

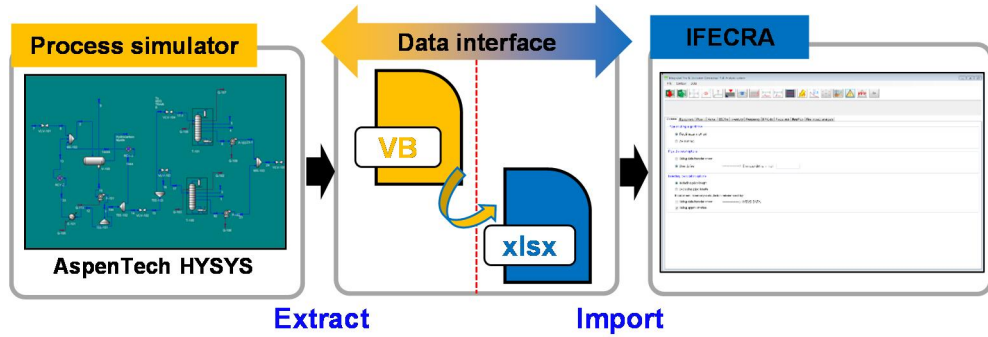


Fig. 12 General outline of data interface between process simulator and IFECRA system

The proposed data transfer sheet which contains FRA input data for equipment, valves and pipes are depicted in Fig. 13. Detailed properties of FRA input data are listed from Table 5 to Table 7 respectively. The IFECRA system reads the proposed data transfer sheet using the developed import module. These FRA input data are automatically stored in the central database of IFECRA system.

In the valve and the pipe data transfer sheet, locations and quantities are calculated using a piping routing algorithm and a valve positioning algorithm respectively. The piping routing algorithm and

valve positioning algorithms are described in details in the following sections.

	A	B	C	D	E	F	G	H	I	J	K	L	M	N	O	P	Q	R	S	T	U	V
	Segment ID	Tag	Equip. ID	Equip. Description	Equip. Type	InstTag	Quantity	Unit	Module	Deck	Leak Rate	COG_X	COG_Y	COG_Z	Mass	Volume	Chn_L	Chn_H	P. Arg.	T °C	CS	
2	SEG_X	Equipment	TOV27961	Cooling Water Expansion Drum	Vessel	XXXXXXXXXXXXXXXXXXXX	1	PS	Top	179400	108600	640176				1620	1620	4150				
3	SEG_X	DUMMY	TOV23110A	Future Item	DUMMY	XXXXXXXXXXXXXXXXXXXX	1	PS	Top	184700	118875	62200				3600	11750	3800				
4	SEG_X	DUMMY	TOV23110B	Future Item	DUMMY	XXXXXXXXXXXXXXXXXXXX	1	PS	Top	178950	118875	62200				3600	11750	3800				
5	SEG_X	DUMMY	TOV7310A	Future Item	DUMMY	XXXXXXXXXXXXXXXXXXXX	1	PS	Top	179700	110400	61100				1200	1800	1200				
6	SEG_X	DUMMY	TOV7310B	Future Item	DUMMY	XXXXXXXXXXXXXXXXXXXX	1	PS	Top	177500	110400	61100				1200	1800	1200				
7	SEG_X	DUMMY	TOV7311A	Future Item	DUMMY	XXXXXXXXXXXXXXXXXXXX	1	PS	Top	181900	110400	61100				1200	1800	1200				
8	SEG_X	DUMMY	TOV7311A	Future Item	DUMMY	XXXXXXXXXXXXXXXXXXXX	1	PS	Top	184100	110400	61100				1200	1800	1200				
9	SEG_X	DUMMY	TOV7312B	Future Item	DUMMY	XXXXXXXXXXXXXXXXXXXX	1	PS	Top	188000	110400	61100				1200	1800	1200				
10	SEG_X	DUMMY	TOV7312A	Future Item	DUMMY	XXXXXXXXXXXXXXXXXXXX	1	PS	Top	180500	110400	61100				1200	1800	1200				
11	SEG_X	Equipment	TOV81910B	Wash Water Cartridge Filter	Vessel	XXXXXXXXXXXXXXXXXXXX	1	PS	Upper	180200	134100	53600				750	750	2125				
12	SEG_X	Equipment	TOV81910A	Wash Water Cartridge Filter	Vessel	XXXXXXXXXXXXXXXXXXXX	1	PS	Upper	188170	134100	53600				750	750	2125				
13	SEG_X	Equipment	TOV28510	H2S Scavenger Buffer Drum	Vessel	XXXXXXXXXXXXXXXXXXXX	1	PS	Upper	195500	104550	53800				4000	11400	17400				
14	SEG_X	Equipment	TOV28510	CST Buffer Drum	Vessel	XXXXXXXXXXXXXXXXXXXX	1	PS	Upper	195600	109550	53800				2420	1000	1000				
15	SEG_X	DUMMY	TOV28511A	Reverse Osmosis Train	DUMMY	XXXXXXXXXXXXXXXXXXXX	1	PS	Upper	188700	121100	54150				3100	8200	4100				
16	SEG_X	DUMMY	TOV28511B	Reverse Osmosis Train	DUMMY	XXXXXXXXXXXXXXXXXXXX	1	PS	Upper	191750	121100	54150				3100	8200	4100				
17	SEG_X	DUMMY	TOV28513	OP Skid for Wash Water Package	DUMMY	XXXXXXXXXXXXXXXXXXXX	1	PS	Upper	196250	113850	54700				4300	4000	5600				
18	SEG_X	DUMMY	TOV28514	Scale inhibitor injection skid	DUMMY	XXXXXXXXXXXXXXXXXXXX	1	PS	Upper	178100	114100	51250				4000	2000	2100				
19	SEG_X	DUMMY	TOV28515	Biocide injection skid	DUMMY	XXXXXXXXXXXXXXXXXXXX	1	PS	Upper	178100	107400	51250				2000	4000	2100				
20	SEG_X	Equipment	TOV9101A	Topside H2S Scavenger Pump	Pump_C	XXXXXXXXXXXXXXXXXXXX	1	PS	Upper	182970	108100	51120				2775	1200	2100				
21	SEG_X	Equipment	TOV9101B	Topside H2S Scavenger Pump	Pump_C	XXXXXXXXXXXXXXXXXXXX	1	PS	Upper	182970	105860	51120				2775	1200	2100				
22	SEG_X	Equipment	TOV9111A	Wash Water Feed Pump	Pump_C	XXXXXXXXXXXXXXXXXXXX	1	PS	Upper	179100	123650	51500				4000	3500	3000				
23	SEG_X	Equipment	TOV9111B	Wash Water Feed Pump	Pump_C	XXXXXXXXXXXXXXXXXXXX	1	PS	Upper	179100	118850	51500				4000	3500	3000				
24	SG	Equipment	TOV22011A	1st Stage Separator	Vessel	TOV22011A-TOE32011A-2A	0.5	PS	Process	187500	122700	44520				19650	4900	4900	12	29.81		
25	SL	Equipment	TOV22011B	1st Stage Separator	Vessel	TOV22011B-TOE32011A-2A	0.5	PS	Process	187500	122700	44520				19650	4900	4900	12	29.78		
26	SG	Equipment	TOV22011C	1st Stage Separator	Vessel	TOV22011C-TOE32011A-2A	0.5	PS	Process	187500	110700	44520				19650	4900	4900	12	29.81		
27	SL	Equipment	TOV22011D	1st Stage Separator	Vessel	TOV22011D-TOE32011B-2B	0.5	PS	Process	187500	110700	44520				19650	4900	4900	11.7	29.78		
28	SEG_X	DUMMY	TOV23110	Flare and H2S Blended Gas Recovery Package	DUMMY	XXXXXXXXXXXXXXXXXXXX	1	PS	Top	219500	119610	62000				7000	12000	4000				
29	SEG_X	Equipment	TOV2321A	Methanol Storage Drum	Vessel	XXXXXXXXXXXXXXXXXXXX	1	PS	Top	210000	119000	62700				3000	10500	3000				
30	SEG_X	Equipment	TOE17001	Fuel Gas Compressor 1 Suction Cooler	Vessel	XXXXXXXXXXXXXXXXXXXX	1	PS	Upper	211740	120700	55475				8910	1420	1420				
31	SEG_X	Equipment	TOE17002	Fuel Gas Compressor 2 Suction Cooler	Vessel	XXXXXXXXXXXXXXXXXXXX	1	PS	Upper	212150	119550	55475				8100	1420	1420				
32	SEG_X	Equipment	TOE17003	Fuel Gas Compressor 2 Discharge Cooler	Vessel	XXXXXXXXXXXXXXXXXXXX	1	PS	Upper	212150	114520	55475				8100	1420	1420				
33	SEG_X	Equipment	TOE17004	Fuel Gas Heater	Vessel	XXXXXXXXXXXXXXXXXXXX	1	PS	Upper	214270	108000	54800				5595	730	730				
34	SEG_X	Equipment	TOE17005	Fuel Gas Heater	Vessel	XXXXXXXXXXXXXXXXXXXX	1	PS	Upper	224270	108100	57800				5595	730	730				
35	SEG_X	Equipment	TOE17006	Fuel Gas Fine Filter	Vessel	XXXXXXXXXXXXXXXXXXXX	1	PS	Upper	220800	111180	57950				1070	1070	3820				
36	SEG_X	Equipment	TOE17007	Fuel Gas Fine Filter	Vessel	XXXXXXXXXXXXXXXXXXXX	1	PS	Upper	220800	111180	54950				1070	1070	3820				
37	SEG_X	Equipment	TOE17008	Fuel Gas Compressor 1	Compressor_C	XXXXXXXXXXXXXXXXXXXX	1	PS	Process	211360	120170	47900				1700	7300	2400				
38	SEG_X	Equipment	TOE17009	Fuel Gas Compressor 2	Compressor_C	XXXXXXXXXXXXXXXXXXXX	1	PS	Process	211360	117170	42820				1550	4200	2200				
39	SEG_X	Equipment	TOE17010	Flare	Flare	XXXXXXXXXXXXXXXXXXXX	1	PS	Process	211360	117170	42820				1550	4200	2200				

Fig. 13 Case example of data transfer sheet

Table 5 Example of equipment data transfer sheet

Equipment sheet			
Segment ID	S510G	Pressure	1.862barg
Type	Equipment	Temperature	112.1C°
Equipment ID	EQ001	C1	0.04
Equipment Description	2 nd Separator	C2	0.875
Equipment Type	Vessel	C3	0.055
End-Tag	EQ001 – EQ003 – PIPE001	C4	0.021
Quantity	1	C5	0.009
Module	S5	C6	0.005
Deck	Upper	C7	0.001
COG X	187500mm	C8	0
COG Y	16000mm	C9	0
COG Z	58700mm	C10	0
Volume	486.72m ³	C11	0
Dimension L	18000mm	Cv	47.58
Dimension W	5200mm	Cp	38.74
Dimension H	5200mm	Cp/Cv	1.76

Table 6 Example of valve data transfer sheet

Valve sheet	
Segment ID	S510G
Type	Valve
Equipment ID	Valve10G
Equipment Description	Chock Valve
Equipment Type	Manual Valve
End-Tag	PIPE001 – Valve10G
Quantity	1
Module	
Deck	
COG X	
COG Y	
COG Z	

Table 7 Example of pipe data transfer sheet

Pipe sheet			
Segment ID		Pressure	1.862barg
Type	Pipe	Temperature	112.1C°
Equipment ID	PIPE001	C1	0.04
Equipment Description		C2	0.875
Equipment Type	Pipe	C3	0.055
End-Tag	EQ001 – EQ003 – PIPE001	C4	0.021
Quantity		C5	0.009
Module		C6	0.005
Deck		C7	0.001
COG X		C8	0
COG Y		C9	0
COG Z		C10	0
Volume		C11	0
Dimension L		Cv	47.58
Dimension W		Cp	38.74
Dimension H		Cp/Cv	1.76

3.3. Central Database of IFECRA System

The central database of IFECRA system collects data from reference layout and process design using the proposed standard data transfer sheet. The IFECRA system automatically stores the data into each class such as equipment, valve and pipe. In equipment, valve and pipe class, length, width, height, COG, volume, quantity, composition and operating conditions are listed. Properties

of each class are summarized from Table 8 to Table 10. Fig. 14 shows the central database of IFECRA system represented in the form of a class diagram.

Table 8 Properties of the equipment class

Equipment	
Properties	Data type
Segment	String
ID	String
Name	String
Equipment Type	String
End-tag	String
Length, Width, Height	Double
COG	Double
Module	String
Deck	String
Quantity	Double
Volume	Double
Operating temperature	Double
Operating pressure	Double
Compositions	List<double>

Table 9 Properties of the valve class

Valve	
Properties	Data type
Segment	String
ID	String
Name	String
Valve Type	String
End-tag	String
Quantity	Double

Table 10 Properties of the pipe class

Pipe	
Properties	Data type
Segment	String
ID	String
Name	String
End-tag	String
Operating temperature	Double
Operating pressure	Double
Compositions	List<double>

The central database of IFECRA system automatically transfers the data to each calculation and simplified model generation module, and general outline of IFECRA system is given in Fig. 11. FRA in pre-FEED stage, the IFECRA system is able to use a 3D geometric model. Therefore, FRA is possible to use a 3D CFD fire simulation to increase FRA accuracy in pre-FEED stage. Every calculation results can be found in a graphical user interface (GUI) of the developed IFECRA system.

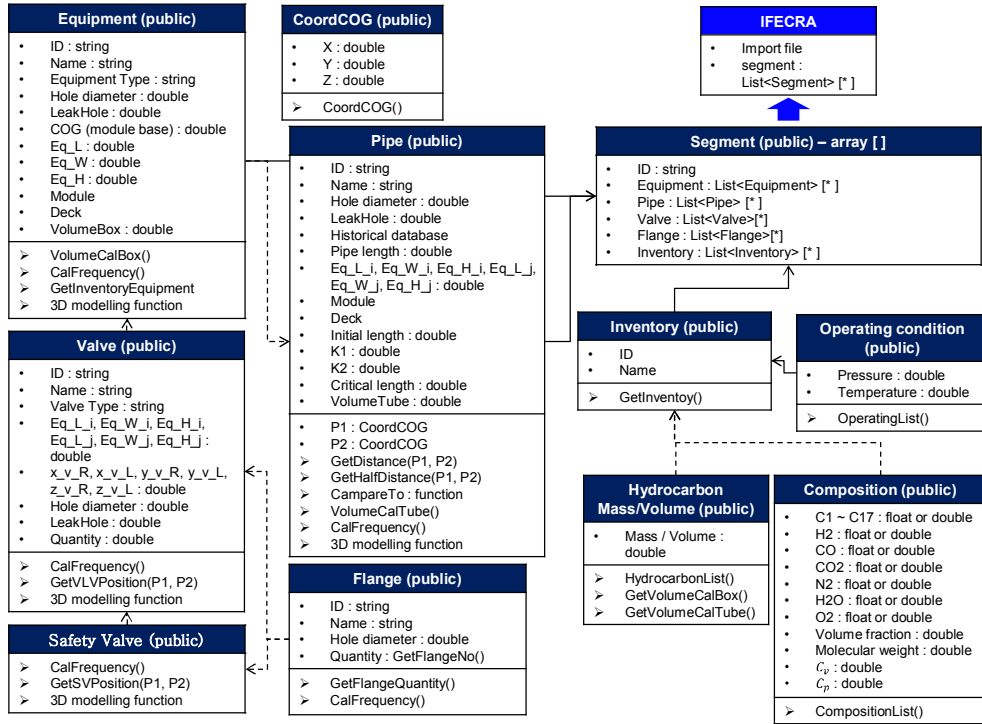


Fig. 14 Central database of IFECRA system expressed by using
class diagram

For the leak frequency calculation from the general FRA case, the piping lengths are estimated roughly. Therefore, there is a large variance in leak frequency calculation results. The IFECRA system not only increases the accuracy of leak frequency calculation, but also decreases the variance because the piping lengths are logically estimated employing a routing algorithm.

A routing algorithm is able to estimate the piping lengths using end-tag information. The end-tag consists of two tags of

equipment to which the pipe is connected, and using the end tag, the 2 connected equipment can be identified, and their information also can be searched. An example is presented in Fig. 15.

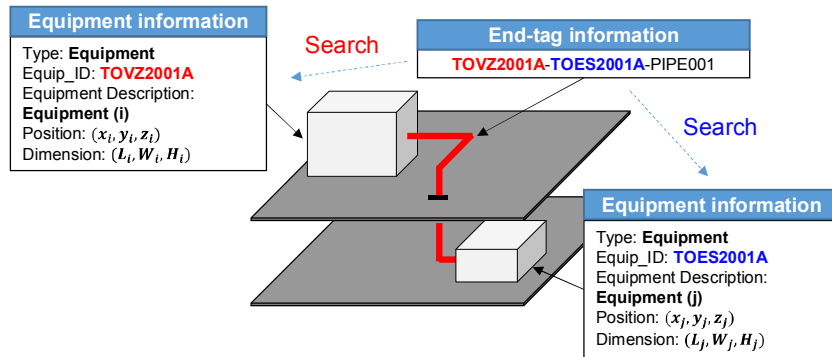


Fig. 15 Systematic description of end-tag information with searched equipment information

In Fig. 15 the 2 equipment can be identified by using the end tag, TOVZ2001A-TOES2001A-PIPE001, which both includes the equipment tags, i.e. TOVZ2001A and TOES2001A. The equipment information contains the type of equipment, equipment ID, description, COG, dimension and so on.

3.3.1. Routing Algorithm: Rectilinear Method

A rectilinear method is a simple routing algorithm and it purposes to find the minimum rectilinear distance between equipment (Kellogg 1956). Procedure of using rectilinear method is shown in Fig. 16. Six nodes are calculated dependent on connection constraints.

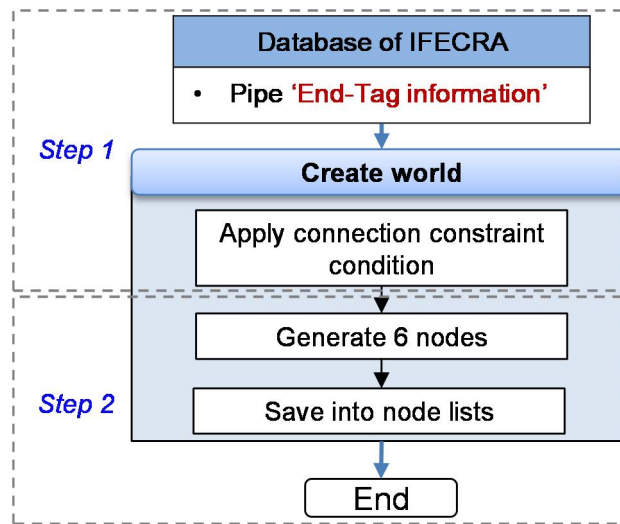


Fig. 16 Routing algorithm by using rectilinear method

The connection constraint conditions in a routing algorithm are visually illustrated in Appendix 7.2. The connection constraint conditions provide the coordinates of the six nodes that are generated based on the location of the equipment. General

procedures of routing algorithm adopting a rectilinear method are summarized as the following steps.

- **Step 1:** Search the information of equipment to which the pipe connects using end-tag information and apply connection constraint conditions.
- **Step 2:** Generate six number of nodes between the equipment. The IFECRA system saves the generated six nodes. Fig. 17 shows an example of the generated six nodes depending on the connection constraint condition,

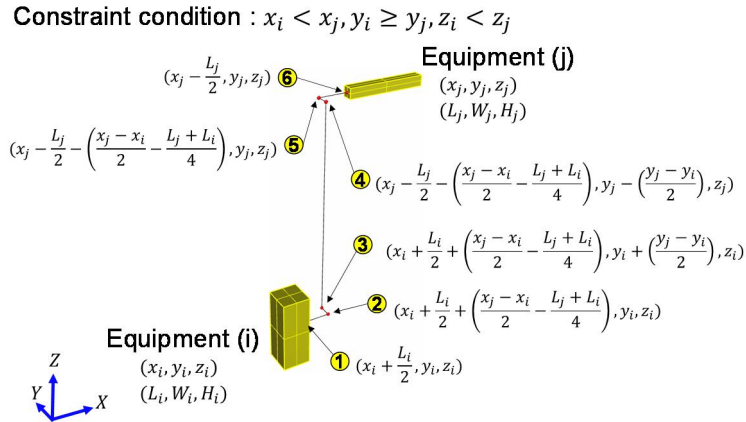


Fig. 17 Example of the generated six nodes depending on connection constraint condition

The piping routing using a rectilinear method can quickly estimate piping length and volume. However, this piping path

overlaps with the surrounding equipment because total six nodes are inherently fixed. An example regarding the problem is shown in Fig. 18 when using the rectilinear method. Therefore, this study considers a path searching algorithm such as A* method.

Fig. 18 Simple example of routing algorithm by using rectilinear method

3.3.2. Routing Algorithm: A* Method

An A* method is a kind of searching algorithm which finds the smallest path cost. The piping path is able to avoid the surrounding equipment using A* method and it makes more realistic (Kim 2014).

Overall procedures of A* method are shown in Fig. 19 and the relevant equation (i.e. heuristic equation) is defined as below.

$$f(n) = g(n) + h(n) + W_{bending}$$

n	= The last node on the path
$f(n)$	= The minimum cost of all routes to the end node via node n
$g(n)$	= The cost of the path from the start node to n
$h(n)$	= The shortest path cost from node n to the end node
$W_{bending}$	= The bending cost

This study selects the cost of the path from the start node to n node as 10. The bending costs is a kind of penalty function, hence the bending cost is carefully determined. The bending cost of this study chooses about 11. In addition, the shortest path cost from node n to the end node uses a rectilinear distance cost shown below.

$$h(n) = |x_{end} - x_n| + |y_{end} - y_n| + |z_{end} - z_n|$$

However, the applied A* algorithm in this study has a limitation. Mainly, the searched path is to just avoid overlapping with other equipment and the path may not be optimal. In order to find the optimal path $h(n)$ should be also calculated as the shortest path without any overlap with equipment. In addition, this algorithm mainly provides the pipe lengths and pipe coordinate points to calculate the leak frequency and to generate a simplified 3D model.

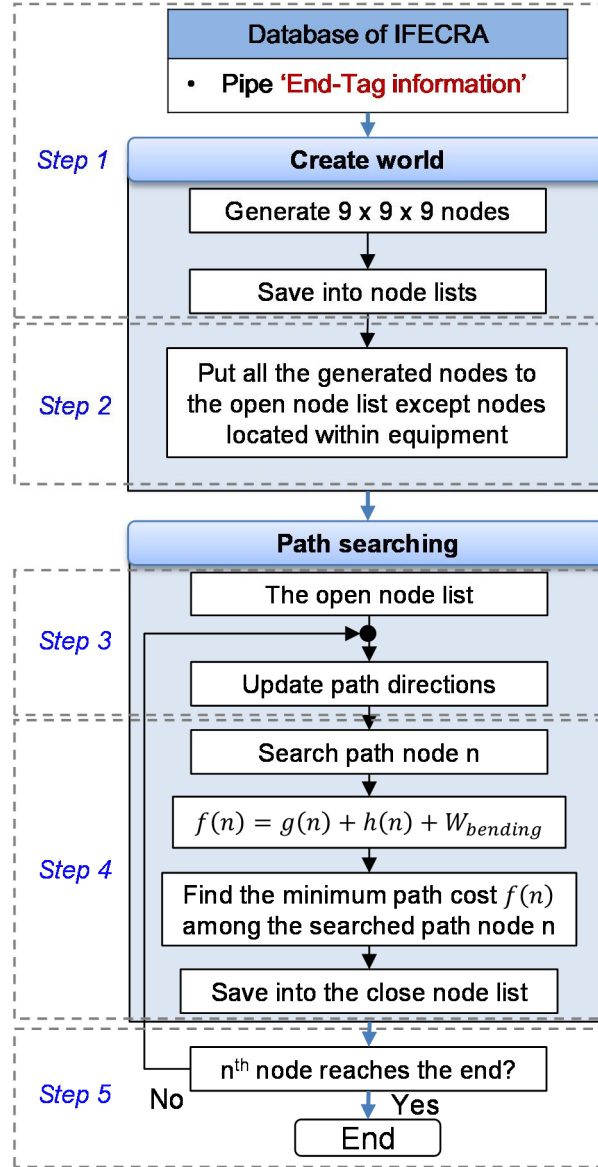


Fig. 19 Routing algorithm by using A* method

In this study, the bending cost is taken into account with the applied A* method to avoid random bending of the path. In addition, the applied A* method of this study only searches 6 path directions

from nth node. Fig. 19 presents a routing algorithm. Before the demonstration of routing algorithm, an “open node lists” and a “close node lists” are briefly defined as follows. An open node lists is represented as a certain number of nodes, with the exception of obstacles. A close node lists is indicated that a piping coordinate is saved as a node. General procedures of routing algorithm using A* method are summarized as follows.

- **Step 1:** Search the information of equipment to which the target pipe connects to, using the end-tag information. In order to apply the routing algorithm, the space between the 2 equipment should be numerically defined, for that a certain number of nodes are introduced to discretize the space. In this study, the number of node is selected as the same, namely, 9 for each direction as shown in Fig. 20, and grid sizes are different in each direction. The applied algorithm can afford to adopt much more nodes, but if the number of node is too large, the computational costs may be highly increased. Finally, the generated nodes are then saved into the node lists of the central database of IFECRA system.

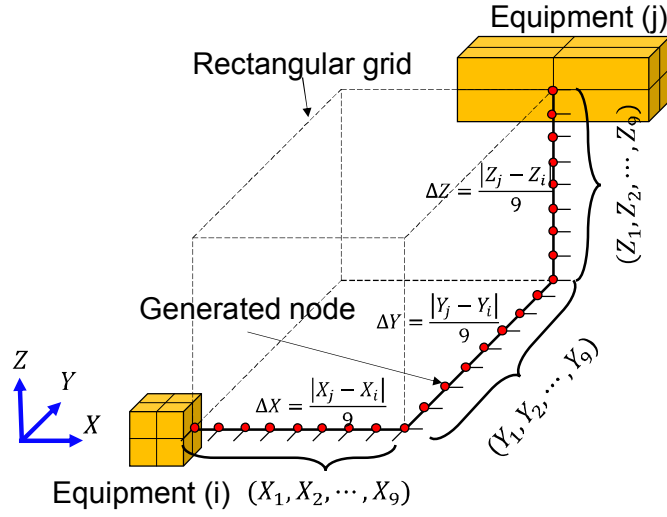


Fig. 20 Example of generated 9 x 9 x 9 nodes in three dimensional
between equipment (i) and equipment (j)

- Step 2:** Determine the obstacles in discretized numerical space presented by the generated nodes. Fig. 21 presents an example of determining the obstacle (e.g. equipment k). If the nodes are located inside the space occupied by the equipment k, these nodes are then regarded as the false nodes. This process is accomplished by the equations ①–③ given in Fig. 21. After identifying all of the false nodes, only the true nodes are saved into open node list from the database of IFECRA system.

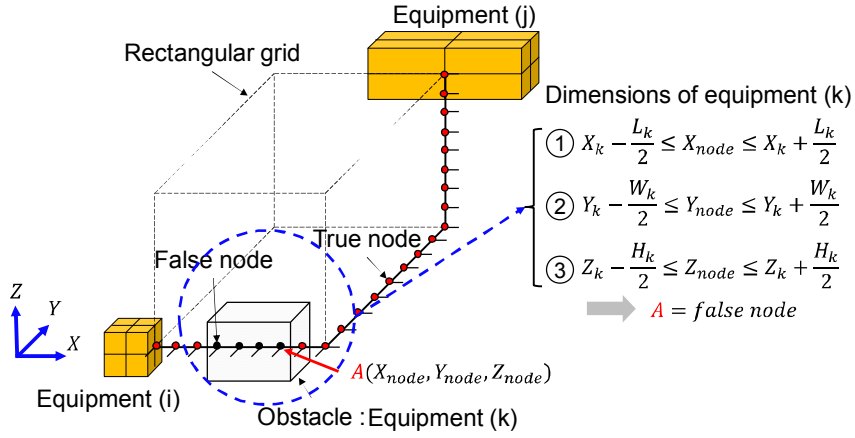


Fig. 21 Example of identifying the presence of obstacles in 729 nodes using the quantified dimension of equipment (k)

- **Step 3:** Search the path directions. In this study, the path directions have a six directions such as leftward, rightward, forward, backward, upward and downward. Fig. 22 shows the selected path directions.

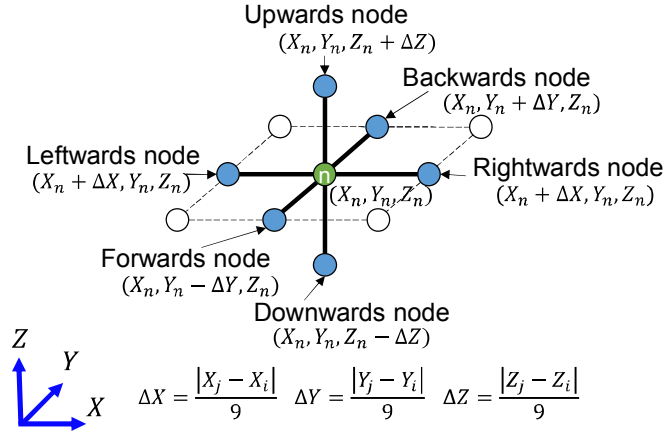


Fig. 22 Presentation of the selected path directions

- **Step 4:** Calculate the minimum path cost from the target node to the end node using the A* equation. Fig. 23 illustrates the bending constraint. From Fig. 23, if the change is made from a single component only from the each searched node (e.g. x-component), the change of which needed to be done in at least three of them, then the bending constraint cannot use in the A* equation. Except this case, the bending constraint can apply to A* equation.

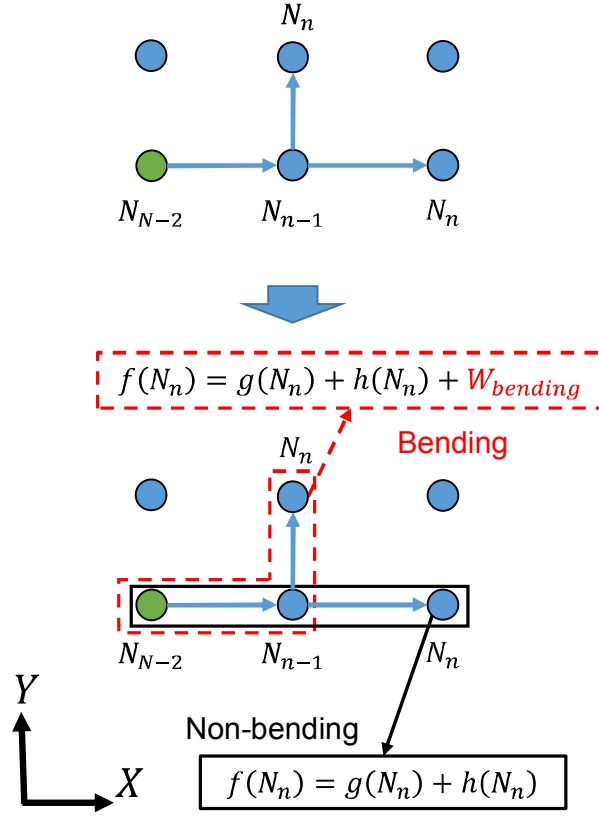


Fig. 23 Illustration of bending constraint

Finally, each path direction (or node) calculates the A* equation, and next path moves to the minimum cost among the calculated path costs and save the node into the close node list.

- **Step 5:** Repeat step 3 and step 4 and calculate piping lengths using the close node list if path node reaches the end.

The piping routing applying A* method can provide more accurate results than a rectilinear method. Fig. 24 presents a simple example of routing results adopting the A* method. A simple example of A* algorithm is demonstrated visually in Appendix 7.3. The both piping algorithms are used in terms of inventory and leak frequency calculations and a simplified 3D model generation in the developed IFECRA system.

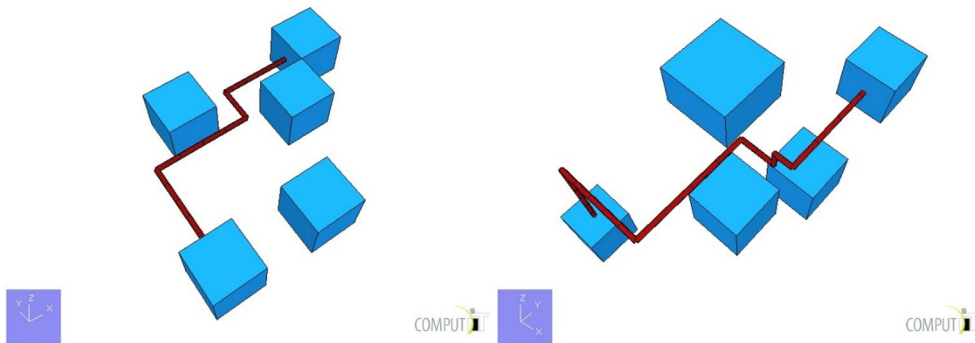


Fig. 24 Simple example of routing algorithm by using A* method

3.3.3. Valve Positioning

The process design such as process flow diagram (PFD), piping & instrument diagram (P&ID) and process simulator (e.g. HYSYS model) is able to provide the quantities of valve. However,

they cannot provide the physical locations such as COG and module location as shown in Fig. 25. However, the developed IFE CRA system is able to calculate the physical positions.

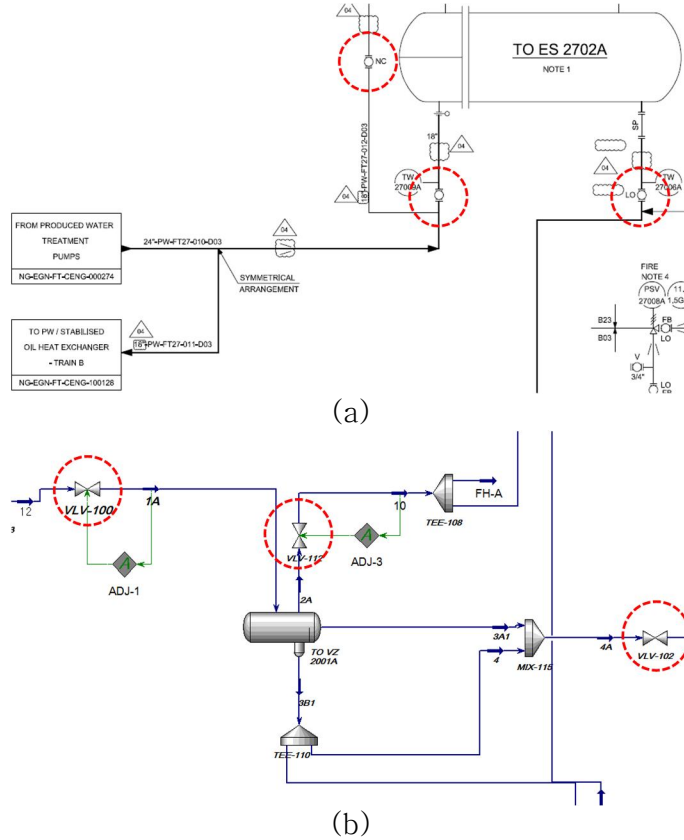


Fig. 25 Case examples of process design (a) PFD/P&ID, and (b) process simulator (e.g. HYSYS).

The valve positioning is used in the leak frequency calculation and a simplified 3D model generation. This study calculates the physical position of the valve through the appropriate assumptions.

General procedures of the valve positioning are summarized in details as follows.

- **Step 1:** Search the information of equipment using the valve end-tag information and collect the pipe close node lists from the central database of IFECRA system.
- **Step 2:** Finds the bending point of the pipe among the pipe close list. For example, when considering a set of the pipe nodes ($Node_s, Node_1, \dots, Node_6$) as shown in Fig. 26 the IFECRA system finds a start node ($Node_s$) and a bending point of the pipe ($Node_3$) using the close pipe node list.

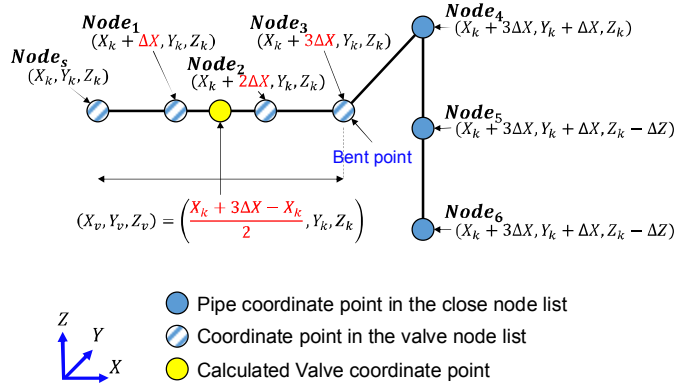


Fig. 26 Example of calculating the valve position

- **Step 4:** Calculate the positions of the ESDV & valve using a start node and a bending point of the pipe. This study

assumes that the ESDV and valve are located in front of equipment. In addition, the location of ESDV and valve is assumed that they are placed at a half-length between the front of the equipment and bent point of the pipe, since the fluid pressure can damage the bent-part of the pipe. Fig. 26 presents an example of calculation of the valve position as mentioned above.

3.4. Inventory Calculation Module

The inventory information such as fuel volume, operating pressure, operating temperature and composition are the input values of consequence modelling in FRA. During the consequence modelling in FRA, the inventory size is determined by the largest equipment of the isolated segment. However, the process design is hard to provide process piping volumes as shown in Fig. 5 and Fig. 25. Hence, most of FRA methods in pre-FEED stage, inventory volume size calculation is takes into account the equipment size only. The inventory volume is important variable to determine the leak duration of fire accident.

Therefore, the developed IFECRA system automatically calculates the inventory volume size of which can combine the equipment size and pipe volume. An accurate estimation of inventory size can increase accuracy of the results because fire simulation is dependent on leak rate and leak duration. Detailed procedures of the inventory calculation algorithm are summarized as follows.

- **Step 1:** Calculate the equipment volumes using the equipment information from the central database of IFECRA system.
- **Step 2:** Calculate the process piping volume that employs the pipe close node list from the central database of IFECRA system.
- **Step 3:** Summate the equipment size and the pipe volume within the boundary of the isolated segment.
- **Step 4:** Find the maximum value of operating pressure and temperature of the equipment to the boundary of the isolated segment.

However, in the current study, for simplicity, the volume of pipe is neglected.

3.5. Leak Frequency Calculation Module

For the leak frequency calculation in general FRA case, the number of equipment is counted manually in the process design. Also, many process designs are required when calculating leak frequency. In addition, process piping length is roughly estimated in the leak frequency calculation because the process design is not able to provide the piping lengths. Hence, the leak frequency calculations have large variance in the results.

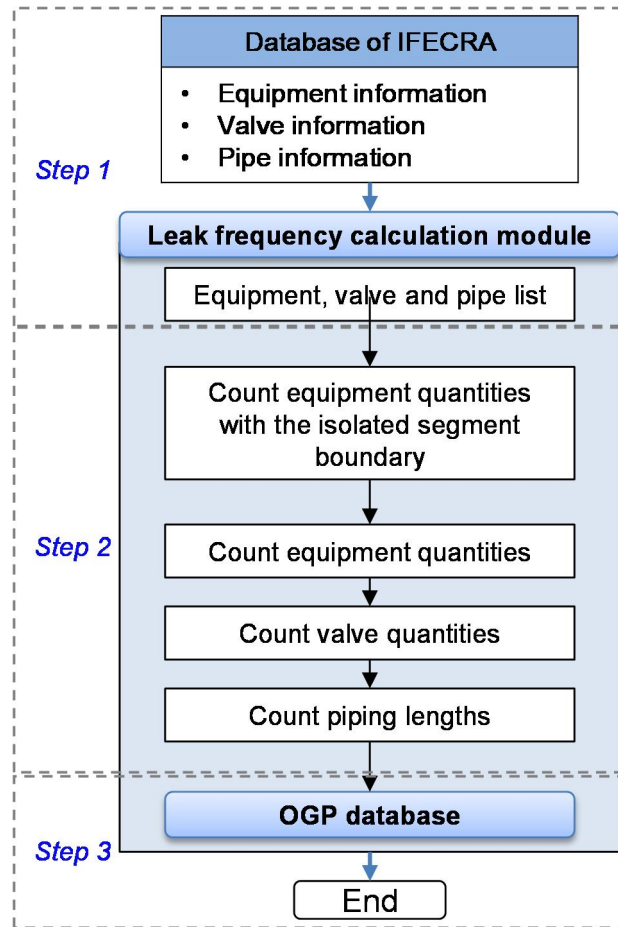


Fig. 27 Leak frequency calculation flowchart

The developed leak frequency calculation module of IFECRA system counts automatically the number of equipment. In addition, the developed module directly estimates the pipe lengths using a routing algorithm. Therefore, the leak frequency calculation module has relatively small variance in results. Moreover, the developed module can increase the efficiency of FRA calculation. Fig. 27

presents the leak frequency calculation flowchart of the applied leak frequency calculation module.

General procedures of leak frequency calculation module are summarized as follows.

- **Step 1:** Identify the equipment, valve and pipe placed at the isolated segment boundary. The equipment, valve and pipe information are automatically transferred from the central database of IFECRA system.
- **Step 2:** Count the number of equipment, valves and pipes, if the isolated segment includes the identified equipment, valves and pipes. The quantities of equipment and valves are automatically transferred from the central database of IFECRA system. The pipe lengths are calculated up to the valve position using the pipe close node list and valve coordinate points. If the coordinate point of valve is not provided, then the pipe length has a half-distance between the equipment.
- **Step 3:** Calculate the leak frequency using the OGP database. The developed IFECRA system stores the historical leak frequency of the OGP database.

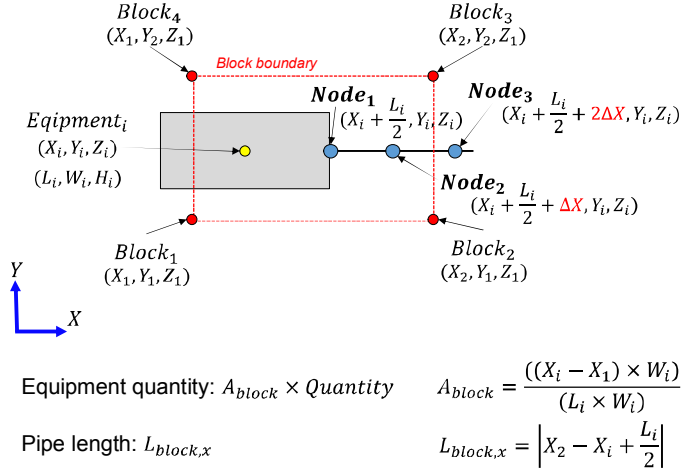


Fig. 28 Example of the leak frequency calculation at the block boundary

Optionally, the leak frequency calculation model calculates the leak frequency at the block boundary. The block boundary can be provided by the coordinate points. Using the coordinate points of block boundary, the system automatically calculates the equipment quantities. In addition, the pipe length is calculated up to the block boundary using the pipe open node lists and the coordinate points of the block boundary. Fig. 28 shows an example of the leak frequency calculation at the block boundary. The quantity of equipment is counted by multiplying the area ratio and quantity as given in Fig. 28. Also, the pipe length is calculated using the pipe open node lists and coordinate point of the block boundary.

3.6. Simplified 3D Generation Module

In most of pre-FEED stages, a 3D geometric model is not available in general FRA case. Hence, a geometric information is not implemented in the risk analysis. An analytical model (e.g. Phast) gives a conservative result of the risk analysis because fire simulation does not reflect geometric information.

This study, however, a simplified 3D geometric model is readily available using a simplified 3D model generation module of the IFECRA system. Hence, the developed IFECRA system is able to use a 3D CFD fire simulation such as Kameleon FireEx (KFX). Therefore, the accuracy of risk analysis can be improved by performing a CFD simulation with a simplified 3D geometric model.

A simplified 3D geometric model is available in KFX which is a commercial software of 3D CFD fire simulation. The KFX geometric model (.kfx) has a text format, hence it easily generates a simplified 3D model by using geometric element commands introduced in KFX user manual (KFX 2010).

From the KFX (2010), the KFX geometric format (.kfx) has four commands that describe geometry and one statement that

groups the geometry primitives into parts. In this study, KFX geometry commands are used in Table 11 below.

Table 11 KFX geometry commands (KFX 2010)

Cylinder Along Coordinate Axis	
Command	CYL: X0 Y0 Z0 RADIUS LENGTH ORIENTATION
X0 Y0 Z0	Coordinates of the starting point (in mm)
LENGTH	Length of cylinder (in mm)
RADIUS	Radius of cylinder (in mm)
ORIENTATION	X, -X, Y, -Y, Z, -Z, i.e. a character denoting which coordinate direction the cylinder is pointing
Skew Cylinder or Cone	
Command	SCYL: X0 Y0 Z0 X1 Y1 Z1 R0 R1
X0 Y0 Z0	Coordinates of the starting point (in mm)
X1 Y1 Z1	Coordinates of the ending point (in mm)
R0	Radius at starting point (in mm)
R1	Radius at ending point (in mm)
Box Oriented Along Axis	
Command	BOX: X0 Y0 Z0 DX DY DZ [P XPH YPH ZPH VPH]
X0 Y0 Z0	Coordinates of the starting point (in mm)
DX DY DZ	Dimensions of box (in mm)
P	If the character P is present, it denotes
XPH YPH ZPH	Optional directional surface porosity for the box
VPH	Optional volume porosity for the box The porosity is a value between 0 and 1, where 0 is fully closed and 1 is filly open
Skew Box	
Command	SBOX: X0 Y0 Z0 X1 Y1 Z1 HEIGHT WIDTH
X0 Y0 Z0	Coordinates of the starting point at the center axis of the box (in mm)
X1 Y1 Z1	Coordinates of the ending point at the center axis of the box (in mm)
HEIGHT	Height of the box (in mm)

WIDTH	Width of the box (in mm)
-------	--------------------------

Based on Fig. 29, an example of a simplified 3D KFX model is in Table 12 utilizing KFX geometry commands.

Table 12 Example format of KFX model based on Fig. 29

Simplified 3D model (.kfx)
//Separator BOX: X_i Y_i Z_i L_i W_i H_i P 0 0 0 0 //Cooler BOX: X_j Y_j Z_j L_j W_j H_j P 0 0 0 0 //Valve01 BOX: V_j V_j V_j 1000 1000 1000 P 0 0 0 0 //Pipe01 SCYL: X_1 Y_1 Z_1 X_2 Y_2 Z_2 L_{12} 156 X SCYL: X_2 Y_2 Z_2 X_3 Y_3 Z_3 L_{23} 156 Y <div style="text-align: center;">\vdots</div> SCYL: X_{n-1} Y_{n-1} Z_{n-1} X_n Y_n Z_n $L_{n-1,n}$ 156 Z

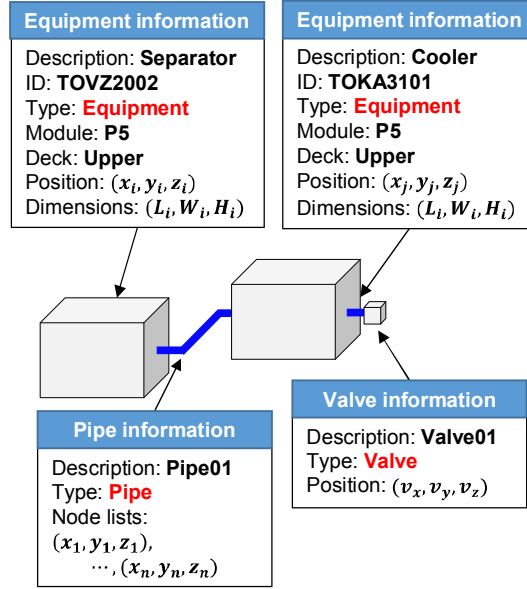


Fig. 29 Systematic description of the developed a 3D model generation module

3.7. Fire Risk Analysis Module

In pre-FEED stage, the fire risk analysis can determine the failure of critical targets based on analytical fire simulation results by hand. Hence, the FRA is inefficiency to determine the fire risk analysis results. Therefore, this study improves efficiency by developing a fire risk analysis module.

The developed fire risk analysis module can automatically determine the failure of critical targets. In addition, the rate of

Passive Fire Protection (PFP) can be automatically provided by adopting the developed module. The fire risk analysis module consists an impact analysis and a risk control. Fig. 30 shows a procedure of the developed fire risk analysis module.

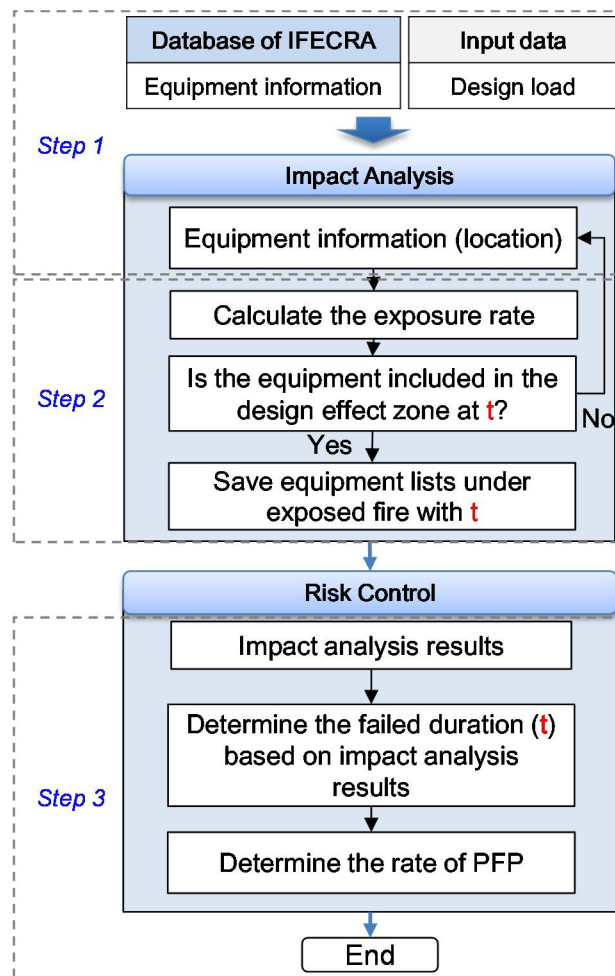


Fig. 30 General procedures of the fire risk analysis module

First of all, the impact analysis determines the failure of critical targets using a design accidental load (DAL). The critical target is identified from the database of IFECRA system. This study proposes the exposure rate. This exposure rate can additionally provide a judgment on the failure of equipment to increase the accuracy. Also, the risk control determines the rate of PFP using the impact analysis results. Detailed procedures of the risk analysis module are summarized as follows.

- **Step 1:** Import design accidental load (DAL) into the IFECRA system and select design criteria (e.g. radiation heat flux level at 37.5kW/m^2).
- **Step 2:** Generate 26 nodes on surface of the equipment. The equipment information can be automatically transferred from the central database of IFECRA system. The radiative heat flux of generated 26 nodes are calculated using a design accidental load (DAL). At this time, the trilinear interpolation method is used to calculate the heat flux of the generated nodes.

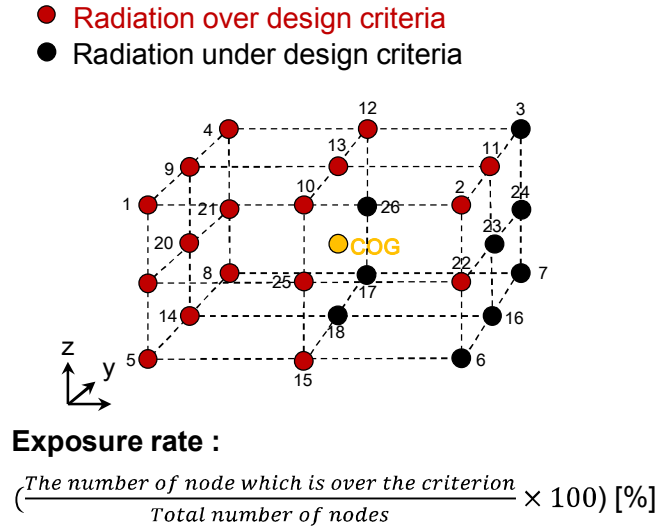


Fig. 31 Example of calculating the exposure rate

If a certain equipment locates in the design effect zone and the exposure rate exceeds the user defined criteria, then the developed module saves the equipment tag and the failure time into the system.

- **Step 4:** Estimate the failure duration and determine the PFP rating based on the impact analysis results.

Fire risk analysis results such as impact analysis and the rate of PFP can be found in the Graphical User Interface (GUI) of the developed IFECRA system.

3.8. User Interface

In this study, the IFECRA system includes the development of the calculation modules such as leak frequency calculation module, simplified 3D model generation module, fire risk analysis module and user interface. Fig. 32 shows the screenshot of the IFECRA system. On the top of user interface, menu bar provides the export of the thermal radiation heat flux contour data. Below the menu, the number of developed module is presented as buttons.

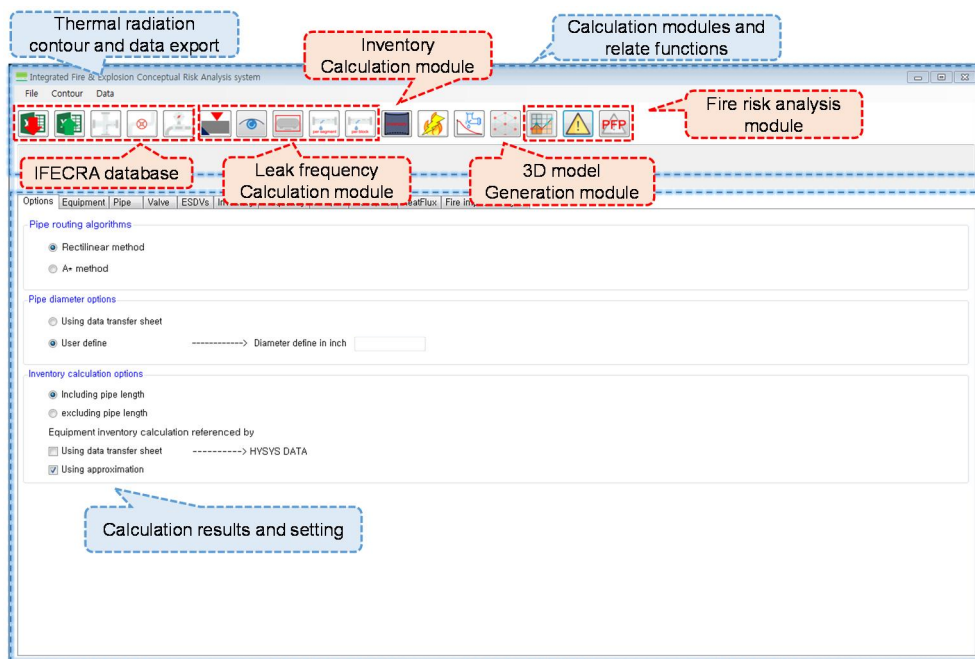


Fig. 32 Screenshot of the IFE CRA system

4. Case Study

4.1. Fire Scenario Identification

Fig. 33 shows a FPSO process area model generated by a simplified 3D model generation module of developed IFECRA system. The process equipment information is defined based on data transfer sheet from the process simulator (e.g. HYSYS). This case study is under the assumption that the HAZID work has already been completed. Therefore, it is determined that the main hazardous inventories in P5 module are the two phase separators (i.e. oil and gas). This case study only considers scenarios related to the jet fire accidents. Also, it is assumed that three kinds of time-dependent leak rate (i.e. large, medium and small) have been calculated according to operating conditions of the identified inventories (Sávio & Asmund 2010) and leak profiles are shown in Fig. 34.

This study selects the main inventory of P5 module using the proposed standard data transfer sheet. Table 13 shows the parameters for the identified scenario with chosen values. The proposed standard data transfer sheet provides the inventory size,

composition, operating pressure and temperature. In this time, the inventory size is only determined by the equipment size.

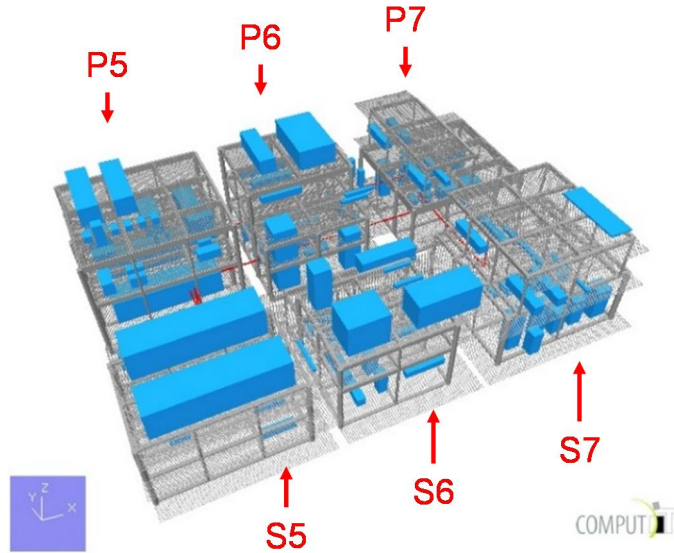


Fig. 33 FPSO process area in case study

Table 13 Parameters for scenario identification

Parameter	Chosen value
Leak rate	Large [65mm], Medium [20mm], Small [5mm]
Leak location	Volumetric center at module P5
Leak direction	10 (left, right, upward, downward, forward, backward, diagonal)
Wind direction	Same as leak direction
Inventory size	187.7m ³
Fuel or composition	CH ₄ (C1 100%)
Operating pressure	12.75bara
Operating temperature	59.31C°

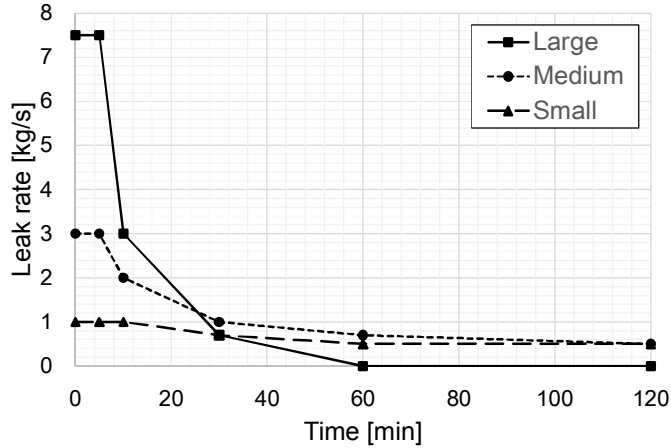


Fig. 34 Time dependent leak profile

The leak rate of hydrocarbon ejected from the process equipment diminishes as time passes because the leak is gradually stopped by the emergency shutdown (ESD) or emergency de-pressurize (EDP) system. Hence, the leak profile is time dependent because leak rate is decreased during the time. Therefore, employing leak profile into fire simulation can lead the dynamic effect of fire accident (Sávio & Asmund 2010). Fig. 34 is the considered leak profile based on leak hole size. In the actual fire accidents on FPSO process area, the leak rate is decayed over the time, and it is commonly called the dynamic (or transient) fire (Sávio & Asmund 2010).

The transient effect of a jet fire has to be because it influences the accuracy of fire simulation. However, if the entire duration of transient fire is considered, the computational time is required too much. Therefore, a simplified transient fire simulation method using a snapshot method is applied in this study to reduce the fire simulation time (see Jin & Jang 2015, Lee et al. 2016).

The leak location places at volumetric center of module P5, and typically 10 leak directions are selected as recommended by FABIG (2009).

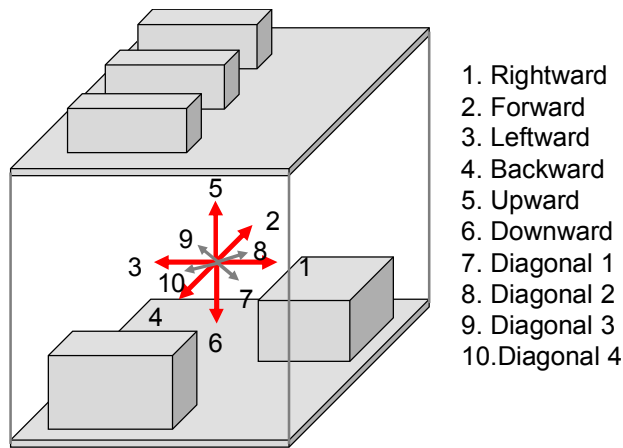


Fig. 35 Selected leak directions

4.1.1. Effective Leak Directions

Leak direction is probabilistically determined because leak directions are inherently random. Leak directions are considered with 10 cases as presented in Fig. 35. If a number of leak direction are increased, then identified fire scenarios are increased. Therefore, it is needed to select effective leak directions in CFD fire simulation.

Fig. 36 shows a fire simulation result. Dotted line indicates that the fire simulation is considered about 10 leak directions. While, the contour presents a result of fire simulation considered 18 leak directions. It is concluded that 10 leak directions are fully enough in this case study.

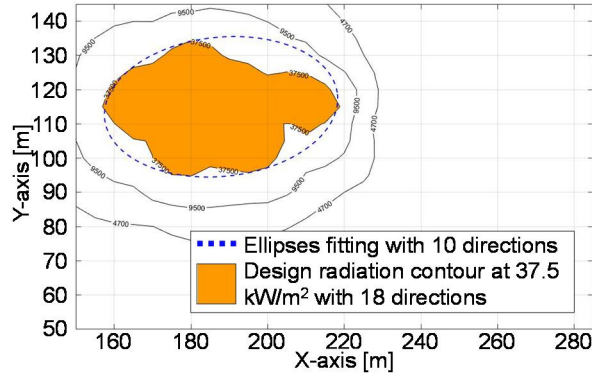


Fig. 36 Fire simulation result comparisons through the number of leak directions

4.2. Leak Frequency Calculation

The leak frequency in module P5 of FPSO process area is calculated using the leak frequency calculation module of the developed IFECRA system. Fig. 37 displays the output of leak frequency calculation results from the developed graphical user interface (GUI).

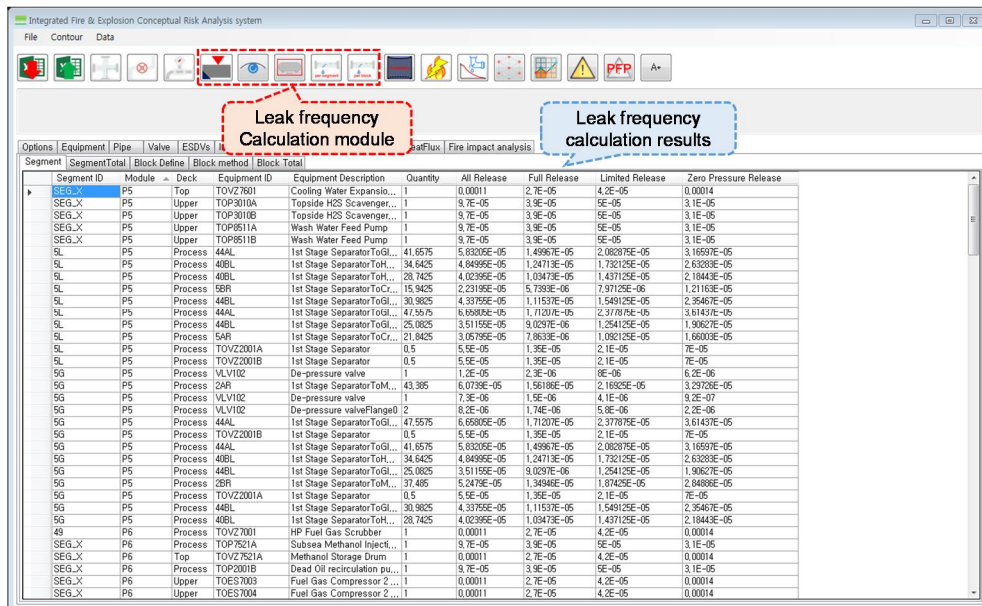


Fig. 37 Leak frequency calculation results by using developed leak frequency calculation module

Table 14 Leak frequency calculation results dependent on leak hole size

Leak frequency		
Small [5mm]	Medium [20mm]	Large [65mm]
1.21E-02	4.58E-03	9.01E-04

Table 14 summarizes the summation of leak frequency calculation results in module P5 of FPSO process area dependent on leak hole size (i.e. large, medium and small).

4.3. Fire Frequency Calculation

The fire frequency of identified fire scenarios are calculated by multiplying leak frequency and ignition probability. The ignition probability used in this case study applies the Cox et al. (1990) ignition model. Detailed descriptions of ignition probability were explained in Chapter 2. The results of ignition probability calculation are given in Table 15. Also, the results of fire frequency calculation are obtained in Table 16.

Table 15 Results of ignition probability calculation by using Cox et al. (1990)

Ignition probability		
Small [5mm]	Medium [20mm]	Large [65mm]
1.58E-02	3.20E-02	5.75E-02

Table 16 Fire frequency calculation results

Fire frequency		
Small [5mm]	Medium [20mm]	Large [65mm]
1.91E-04	1.46E-04	5.18E-05

4.4. Fire Simulation

4.4.1. Radiation Calculation

This study, the fire simulation is carried out using the Kameleoaon FireEx (KFX) software. KFX is the most advanced fire simulator which is available to reflect the turbulent combustion flow using the Eddy Dissipation Concept proposed by Magnussen and Hjertager (1976), and simultaneously calculate the radiation heat flux employing the Discrete Transfer Model (DTM) proposed by Shah and Lockwood (1979). The basic concept of DTM is that radiation exchange is calculated by integration of radiation absorption and emittance along a huge number of rays throughout the calculation domain (KFX 2010). The accuracy is depended by the number of ray that goes through the flame such as the given in Fig. 38.

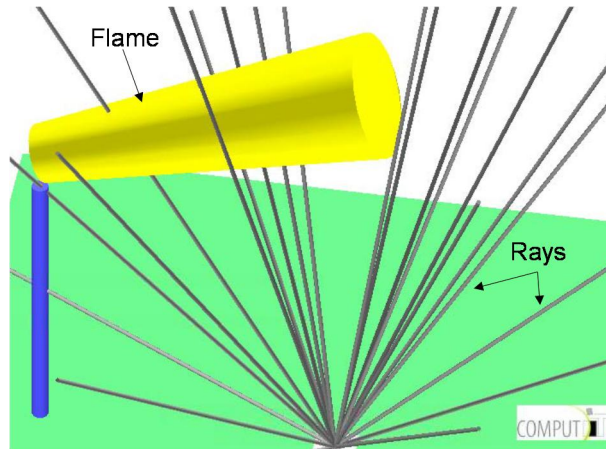


Fig. 38 Radiation flux calculated in one grid point [13]

This study briefly explains a physical concept of radiation heat flux calculation. Radiation intensity I for certain direction is defined as a rate of radiation energy emission or absorption per unit area normal to the direction, unit solid angle of the direction, unit wave length and unit time (Siegel & Howell 1992). The equation of radiation intensity is given in below.

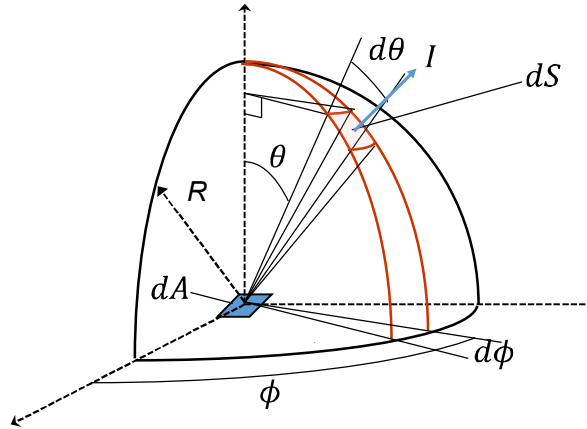


Fig. 39 Radiation intensity (ray) and solid angle

For solid angle

$$d\omega = \frac{dS}{R^2} = \sin\theta d\theta d\phi$$

Radiation intensity

$$I(\lambda, \theta, \phi) = \frac{d^4Q}{dA \cos\theta d\lambda d\omega dt}$$

I = Radiation intensity

Q = Energy rate; energy per unit time

A = Surface area

λ = Wave length

DTM is used for calculating the radiation intensity for all directions over sphere. Furthermore, the obtained radiation intensities are used for calculating radiation heat flux through mathematical integrations over sphere.

In KFX, radiation heat flux calculation is carried out by using the bullet monitor. Bullet monitor is a virtual small ball spread over the entire domain and its surface is discretized by proper number of solid angle for logging the entire radiative intensities such as Fig. 40.

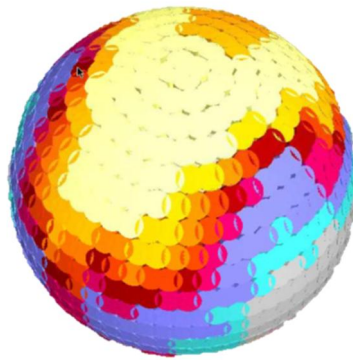


Fig. 40 Visualized the bullet monitor with the calculated radiation intensity (KFX 2010)

This study, the bullet monitor points are placed in a regular grid pattern such as given in Fig. 41. Table 17 presents the input data used for setting the bullet monitor points in KFX.

Table 17 Properties of bullet monitor setting in KFX

Variable	Chosen value
Number of ordinates (rays)	500
Adaptive trace	On
Lower corner (X)	150m
Node distance (dX)	5m
Number of nodes (X)	28
Lower corner (Y)	50m
Node distance (dY)	5m
Number of nodes (Y)	20
Lower corner (Z)	32m
Node distance (dZ)	5m
Number of nodes (Z)	12
Total bullet monitor points	$28 \times 20 \times 12 = 6720$

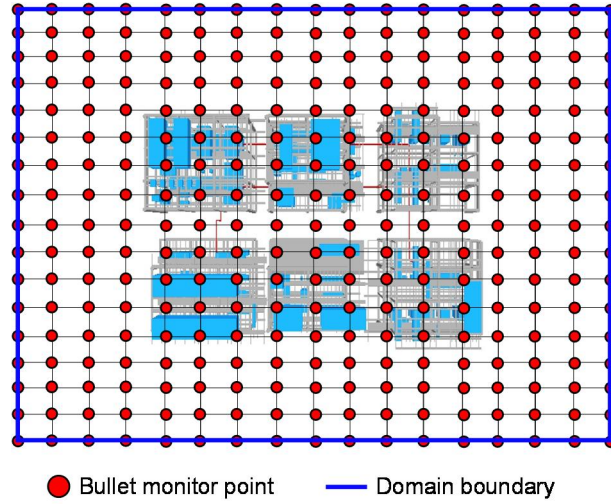
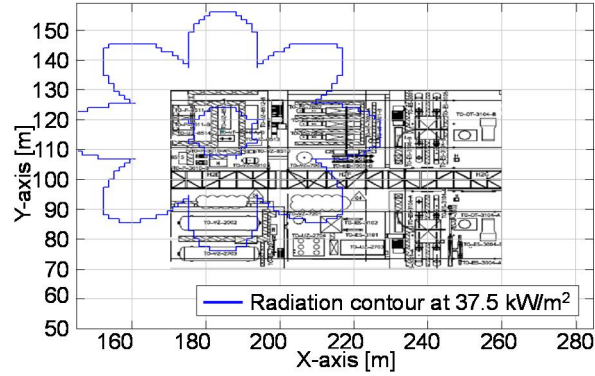


Fig. 41 Bullet monitor points to obtain the radiative heat flux around FPSO topside process area

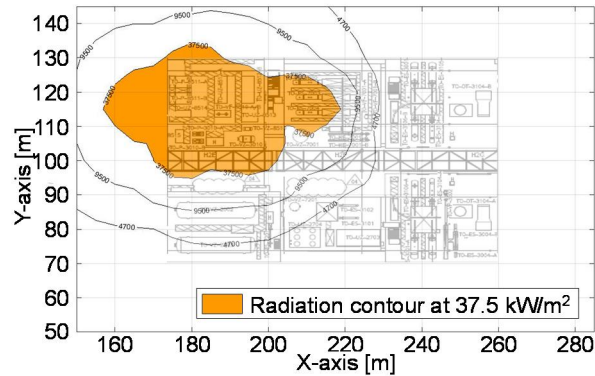
4.4.2. Fire Simulation Result

In this case study, a fire accident is simulated by both analytical model (e.g. Phast) and 3D CFD model (i.e. KFX) to compare the radiation heat flux contour results. First of all, the fire simulation result is compared between the CFD model and the analytical model respectively. Also, the fire simulation result analyzes the comparison between CFD model without the 3D geometric model and analytical model.

Fig. 42 presents the radiation heat flux contour of fire simulation using the both analytical and CFD model respectively.



(a)



(b)

Fig. 42 Radiation heat flux contour comparison between (a) analytical model (Phast) and (b) CFD model (KFX)

According to the consequences of fire simulation, it is obviously concluded that geometric model has a significant effect on the fire consequence as given in Fig. 43. For this reason, the area

of radiation heat flux contour in analytical model is bigger than CFD model.



Fig. 43 Jet fire flame interaction with surrounding equipment in CFD
fire simulation

Fig. 44 shows a case example of radiation heat flux contour comparison of the analytical model (e.g. Phast) and CFD model (e.g. KFX). In this time, the geometric model is not applied in CFD model. For this fire simulation result, the radiation heat flux contours seem similar distributions.

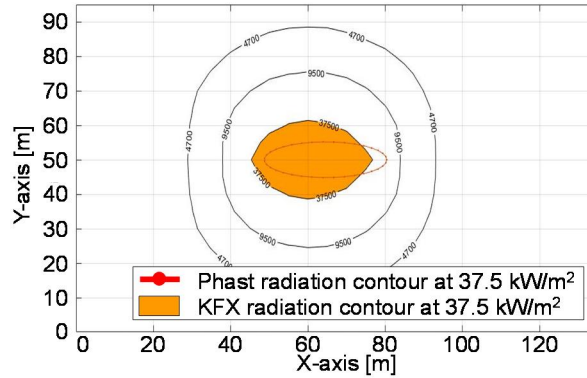


Fig. 44 Radiation heat flux contour comparison both analytical model and CFD model without geometry

4.5. Risk Analysis

4.5.1. Design Criterion

A set of design (i.e. impact) criterion is used to evaluate the critical target. The set of applicable criteria for the impact on critical targets is dependent on radiation levels, based on assumption by Total (2009).

- The thermal radiation level which can impair the escape routes is considered to at 4.7kW/m^2 .
- The thermal radiation level at 9.5kW/m^2 is considered to fire zoning considerations in FRA and 1% lethality for QRA.

- The thermal radiation level at 37.5kW/m^2 is selected for assessment of damage to equipment.

The fire consequences consider the impact of the potential fires on FPSO performed on a module by module basis. The failure time of critical target is used by evaluating the impact analysis and the failure time is indicated in Table 18.

Table 18 Design criterion for each critical target with failure time

Critical target	Failure time
Adjacent flexible risers	5 minutes
Process vessel	5 minutes
Piperack	5 minutes
Module supports	10 minutes
Flare tower	10 minutes
Crane pedestal	10 minutes
Hull deck	15 minutes
FPSO hull side	20 minutes
E & I buildings	10 minutes
Living quarters	10 minutes
Fire water pump enclosures	10 minutes
Fire water caissons	10 minutes
Flare KO drums	5 minutes
Secondary muster shelter	5 minutes

In case study, a level of radiation is selected about 37.5kW/m^2 for evaluating the failure of equipment (i.e. impact analysis).

4.5.2.Design Effect Zone

The design effect zone is possible to identify the failure of critical targets. For KFX, it is not available to draw a circle because KFX does not calculate the flame size. However, KFX can select the monitoring points over the entire calculation domain. Hence, the detailed procedures of determining the design effect zone in KFX can be summarized as follows.

- Obtain the exceedance curve combining radiation heat flux values determined from monitoring points and fire frequency.
- Calculate the design radiation heat flux values according to the design acceptance criterion.
- Obtain the design radiation contour using design radiative heat flux values.
- Fits a curve to the design radiation contour employing the least squares ellipse fitting method.

Fig. 45 shows the above procedures visually, and the 6720 monitoring points are selected over the entire calculation domain in this case study. In this time, the monitoring points can be

represented by the bullet monitoring points as described in Section 4.4.

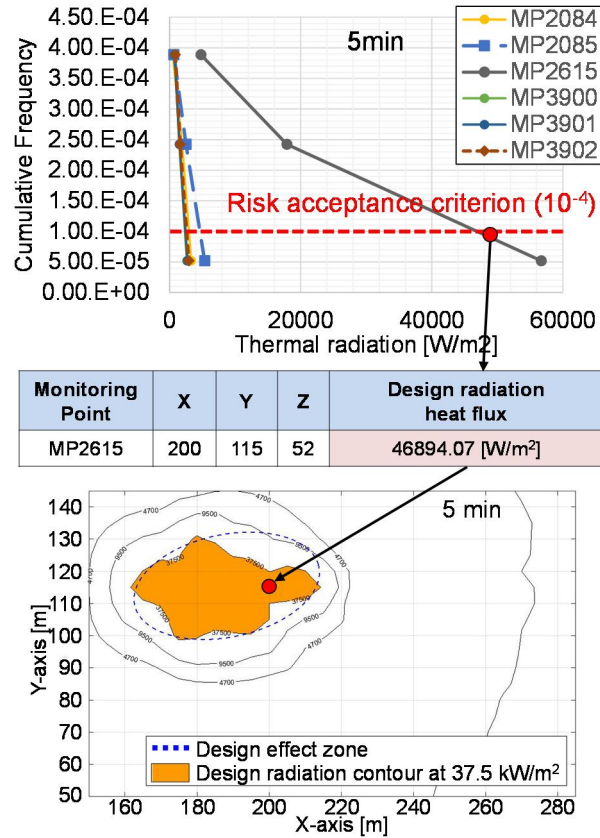


Fig. 45 Example procedures of determining the design effect zone by using radiation heat flux data from monitoring points

The level of radiation contour about 37.5kW/m² is used, and design effect zones for each time are shown from Fig. 46 to Fig. 50.

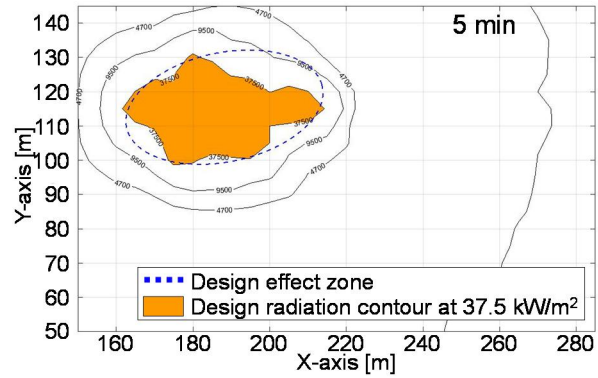


Fig. 46 Design radiation contour and effect zone at 5 minutes

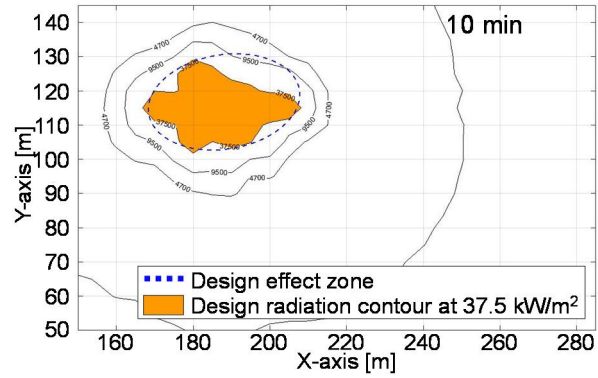


Fig. 47 Design radiation contour and effect zone at 10 minutes

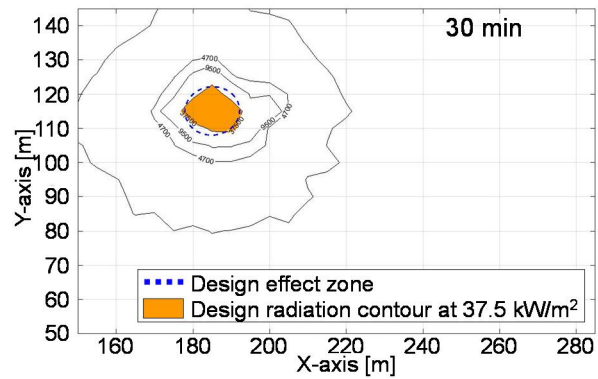


Fig. 48 Design radiation contour and effect zone at 30 minutes

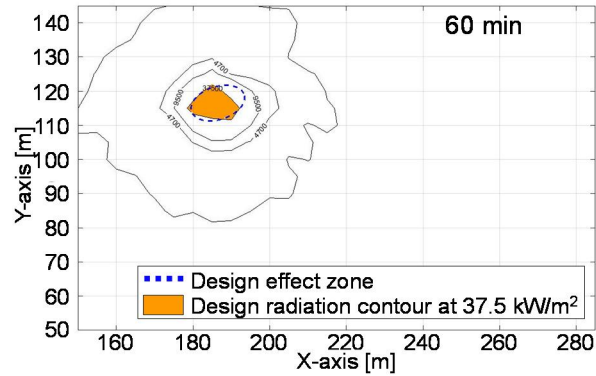


Fig. 49 Design radiation contour and effect zone at 60 minutes

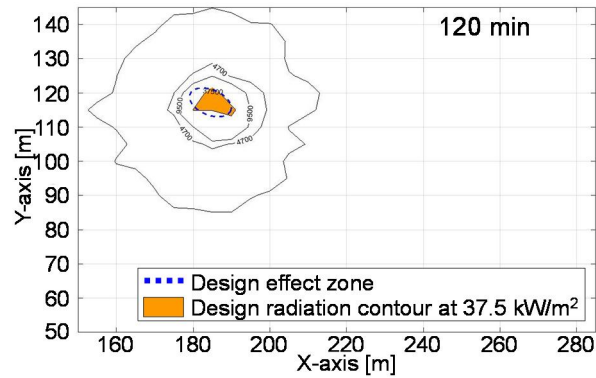


Fig. 50 Design radiation contour and effect zone at 120 minutes

4.5.3. Design Effect Zone Comparison

The design effect zones are compared to the analytical model and the CFD model. The design effect zone used in Phast is described in Chapter 2. Design effect zones are shown from Fig. 51

to Fig. 55. The comparisons are clearly shown that the design effect zone resulted from the analytical model (e.g. Phast) is obtained bigger area than the CFD model (e.g. KFX).

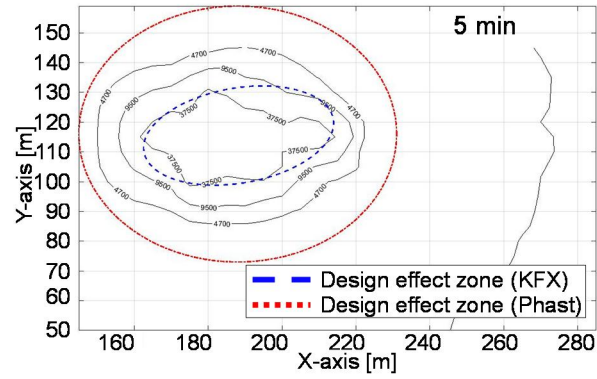


Fig. 51 Design effect zones at 5 minutes between KFX and Phast

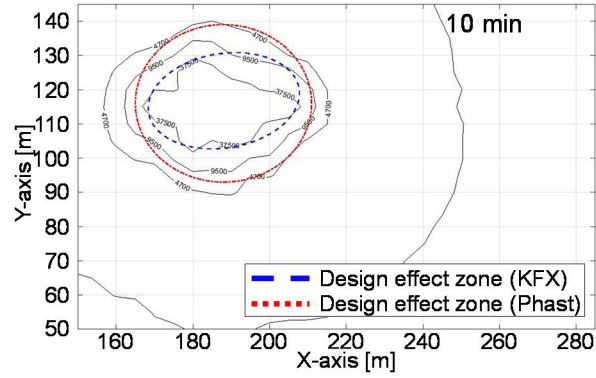


Fig. 52 Design effect zones at 10 minutes between KFX and Phast

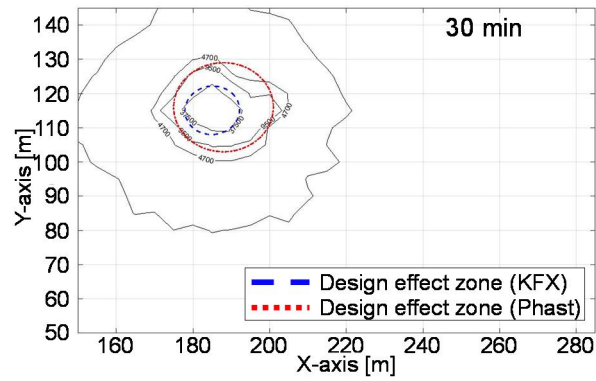


Fig. 53 Design effect zones at 30 minutes between KFX and Phast

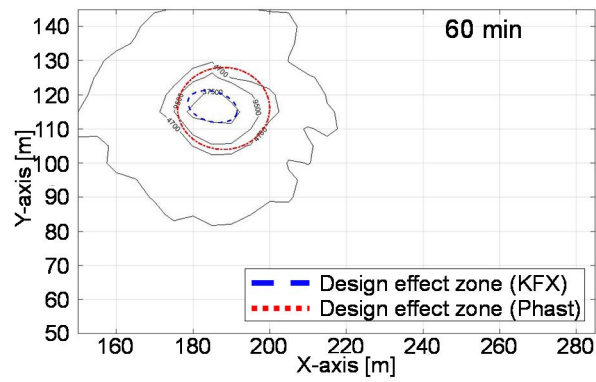


Fig. 54 Design effect zones at 60 minutes between KFX and Phast

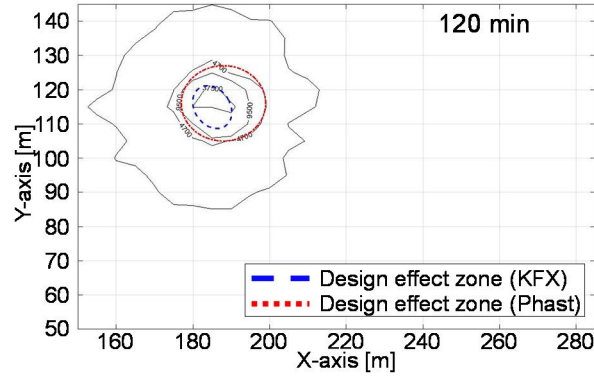


Fig. 55 Design effect zones at 120 minutes between KFX and Phast

4.5.4. Impact Analysis Results

The failure of critical target is determined by the design effect zone. The failure of critical target is checked by comparing a target location and a contour of specific radiation level (i.e. design effect zone). The fire risk analysis module of the developed IFECRA system automatically determines the failure of critical targets. In this study, the results of failure target can be found in the developed graphical user interface (GUI).

ID	Description	Type	Module	Deck	5 min.	10 min.	30 min.	60 min.	120 min.	min.
TOV2300	Cooling Water Expansion Drum	Vessel	P5	Top						
TOVF9510B	Wash Water Cartridge Filter	Vessel	P5	Upper	Exposed	Exposed	Exposed	Exposed	Exposed	
TOVF9510A	Wash Water Cartridge Filter	Vessel	P5	Upper	Exposed	Exposed	Exposed	Exposed	Exposed	
TOVZ3010	H2S Scavenger Buffer Drum	Vessel	P5	Upper	Exposed	Exposed	Exposed	Exposed	Exposed	
TOVZ9510	CST Buffer Drum	Vessel	P5	Upper	Exposed	Exposed	Exposed			
TOP3010A	Topside H2S Scavenger Pump	Pump.C	P5	Upper	Exposed	Exposed	Exposed			
TOP3010B	Topside H2S Scavenger Pump	Pump.C	P5	Upper	Exposed	Exposed	Exposed			
TOP9511A	Wash Water Feed Pump	Pump.C	P5	Upper	Exposed	Exposed	Exposed			
TOP9511B	Wash Water Feed Pump	Pump.C	P5	Upper	Exposed	Exposed	Exposed			
TOVZ2001A	1st Stage Separator	Vessel	P5	Process						
TOVZ2001B	1st Stage Separator	Vessel	P5	Process	Exposed					
TOVZ2001B	1st Stage Separator	Vessel	P5	Process	Exposed					
TOVZ7521A	Methanol Storage Drum	Vessel	P6	Top	Exposed					
TOES7002	Fuel Gas Compressor 1 Suction Cooler	Vessel	P6	Upper						
TOES7003	Fuel Gas Compressor 2 Suction Cooler	Vessel	P6	Upper						
TOES7004	Fuel Gas Compressor 2 Discharge Cooler	Vessel	P6	Upper	Exposed					
TOHE7001A	Fuel Gas Heater	Vessel	P6	Upper						
TOHE7001B	Fuel Gas Heater	Vessel	P6	Upper						
TOVF7001A	Fuel Gas Fine Filter	Vessel	P6	Upper						
TOVF7001B	Fuel Gas Fine Filter	Vessel	P6	Upper						
TOKA7001	Fuel Gas Compressor 1	Compressor.C	P6	Process						
TOKA7002	Fuel Gas Compressor 2	Compressor.C	P6	Process						
TOP2001A	Dead Oil recirculation pump	Pump.C	P6	Process						
TOP2001B	Dead Oil recirculation pump	Pump.C	P6	Process						
TOP7521A	Subsea Methanol Injection Pump	Pump.C	P6	Process						
TOP7521B	Subsea Methanol Injection Pump	Pump.C	P6	Process						
TOP7524A	Topside Methanol Injection Pump	Pump.C	P6	Process						
TOP7533A	Topside Methanol Injection Pump	Pump.C	P6	Process						

Fig. 56 The impact analysis results by using the fire risk analysis of developed IFECRA system

Fig. 57 illustrates an example of the impact analysis results between KFX and Phast. The critical target TOES 7004 is located in a circle with design effect zone at 5 minutes. However, at 10 minutes, TOES 7004 is only placed inside a circle in design effect zone employed Phast. From Table 19 to Table 21 show the results of impact analysis.

Module P5 is the place where a fire accident is occurred, therefore the most of equipment are exposed under the fire accident. In module P6 and S5 which are located within a short

distance from module P5, the most of equipment are exposed to the fire when the analytical model (e.g. Phast) is used. However, a few equipment are exposed under the fire when the CFD model (e.g. KFX) is used.

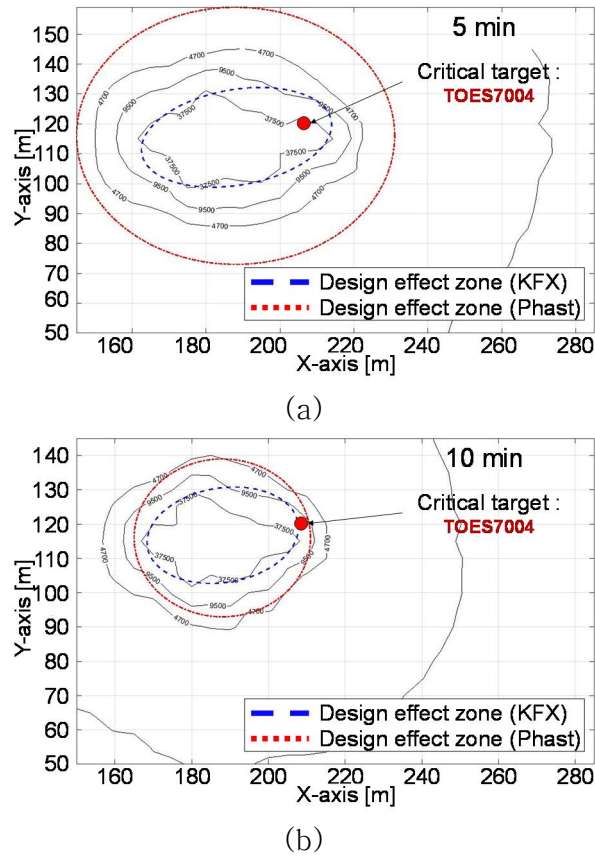


Fig. 57 Impact analysis comparison between KFX and Phast (a)

Design effect zone with critical target at 5 minutes (b) Design effect zone with critical target at 10 minutes

Table 19 Impact analysis result comparisons in module P5

ID	Descriptions	Type	Module		5min		10min		30min		60min		120min	
TOVZ7601	Cooling Water Expansion Drum	Vessel	P5	Top		●		●						
TOVF8510B	Wash Water Cartridge Filter	Vessel	P5	Upper	○	●	○	●	○	●	○	●	○	●
TOVF8510A	Wash Water Cartridge Filter	Vessel	P5	Upper	○	●	○	●	○	●	○	●	○	●
TOVZ3010	H2S Scavenger Buffer Drum	Vessel	P5	Upper	○	●	○	●						
TOVZ8510	CST Buffer Drum	Vessel	P5	Upper	○	●	○	●	○	●		●		
TOP3010A	Topside H2S Scavenger Pump	Pump	P5	Upper	○	●	○	●	○	●		●		●
TOP3010B	Topside H2S Scavenger Pump	Pump	P5	Upper	○	●	○	●		●				
TOP8511A	Wash Water Feed Pump	Pump	P5	Upper	○	●	○	●						
TOP8511B	Wash Water Feed Pump	Pump	P5	Upper	○	●	○	●	○	●		●		
TOVZ2001A	1st Stage Separator	Vessel	P5	Process		●		●						
TOVZ2001A	1st Stage Separator	Vessel	P5	Process		●		●						
TOVZ2001B	1st Stage Separator	Vessel	P5	Process	○	●		●		●				
TOVZ2001B	1st Stage Separator	Vessel	P5	Process	○	●		●		●				
Note: ○ : Exposed to fire obtained by using CFD model (e.g. KFX) ● : Exposed to fire obtained by using analytical model (e.g. Phast)														

Table 20 Impact analysis result comparisons in module P6

ID	Descriptions	Type	Module		5min		10min		30min		60min		120min	
TOVZ7521A	Methanol Storage Drum	Vessel	P6	Top	○	●								
TOES7002	Fuel Gas Compressor 1 Suction Cooler	Vessel	P6	Upper		●		●						
TOES7003	Fuel Gas Compressor 2 Suction Cooler	Vessel	P6	Upper		●		●						
TOES7004	Fuel Gas Compressor 2 Discharge Cooler	Vessel	P6	Upper	○	●		●						
TOHE7001A	Fuel Gas Heater	Vessel	P6	Upper		●								
TOHE7001B	Fuel Gas Heater	Vessel	P6	Upper		●								
TOVF7001A	Fuel Gas Fine Filter	Vessel	P6	Upper		●								
TOVF7001B	Fuel Gas Fine Filter	Vessel	P6	Upper		●								
TOKA7001	Fuel Gas Compressor 1	Vessel	P6	Process		●								
TOKA7002	Fuel Gas Compressor 2	Vessel	P6	Process		●								
TOP2001A	Dead Oil recirculation Pump	Pump	P6	Process		●								
TOP2001B	Dead Oil recirculation Pump	Pump	P6	Process		●								
TOP7521A	Subsea Methanol Injection Pump	Pump	P6	Process		●								
TOP7521B	Subsea Methanol Injection Pump	Pump	P6	Process		●								

TOP7524A	Topsides Methanol Injection Pump	Pump	P6	Process		●								
TOP7533A	Topsides Methanol Injection Pump	Pump	P6	Process		●								
TOVF7525A	Subsea Methanol Injection Filter A	Vessel	P6	Process		●								
TOVF7525B	Subsea Methanol Injection Filter B	Vessel	P6	Process		●								
TOVZ7001	HP Fuel Gas Scrubber	Vessel	P6	Process	○	●								
TOVZ7002	LP Fuel Gas Scrubber	Vessel	P6	Process		●								
TOVZ7003	Fuel Gas Compressor 1 Suction Scrubber	Vessel	P6	Process		●		●						
TOVZ7004	Fuel Gas Compressor 2 Suction Scrubber	Vessel	P6	Process		●		●						
Note: ○ : Exposed to fire obtained by using CFD model (e.g. KFX) ● : Exposed to fire obtained by using analytical model (e.g. Phast)														

Table 21 Impact analysis result comparisons in module S5

ID	Descriptions	Type	Module		5min		10min		30min		60min		120min	
TOVZ2703	Produced Water Skimmer Degassing Drum	Vessel	S5	Upper										
TOVZ2002	2nd Stage Separator	Vessel	S5	Upper		●								
TOVZ2002	2nd Stage Separator	Vessel	S5	Upper		●								
TOES7201	Dump Cooler	Vessel	S5	Upper										
TOES2702A	Produced Water / Stabilized Oil Heat Exchanger	Vessel	S5	Mezzanine		●								
TOES2702B	Produced Water / Stabilized Oil Heat Exchanger	Vessel	S5	Mezzanine		●								
TOES2001B2	Crude Oil Heater	Vessel	S5	Mezzanine		●								
TOES2001A 2	Crude Oil Heater	Vessel	S5	Mezzanine		●								
TOES2001A 1	Crude Oil Heater	Vessel	S5	Mezzanine		●								
TOES2001B1	Crude Oil Heater	Vessel	S5	Mezzanine		●								
TOES2101	Wash Water Heater	Vessel	S5	Mezzanine		●								
TOES2002	Dead Oil Heater	Vessel	S5	Mezzanine		●								

				e										
TOP2703C	Produced Water Treatment Pumps	Pump	S5	Process		●								
TOP2703B	Produced Water Treatment Pumps	Pump	S5	Process		●								
TOEP2501B	Stabilized Oil Cooler	Vessel	S5	Process		●								
TOEP2501A	Stabilized Oil Cooler	Vessel	S5	Process		●								
TOP2001D	Dead Oil Recirculation Pump	Pump	S5	Process		●								
TOP2703A	Produced Water Treatment Pumps	Pump	S5	Process		●								
TOP2001C	Dead Oil Recirculation Pump	Pump	S5	Process		●								
Note: ○ : Exposed to fire obtained by using CFD model (e.g. KFX) ● : Exposed to fire obtained by using analytical model (e.g. Phast)														

4.6. Risk Control

4.6.1. Passive Fire Protection Rating Results

The rate of Passive Fire Protection (PFP) is determined by the developed fire risk analysis module of IFECRA system. For example, the critical target TOES 7004 is exposed to jet fire during 5 minutes using CFD model (e.g. KFX). However, the critical target TOES 7004 is exposed to jet fire during 10 minutes using analytical model (e.g. Phast). Based on results of impact analysis, the rate of PFP can be obtained. Table 22 to Table 23 list the results for determining the rate of PFP.

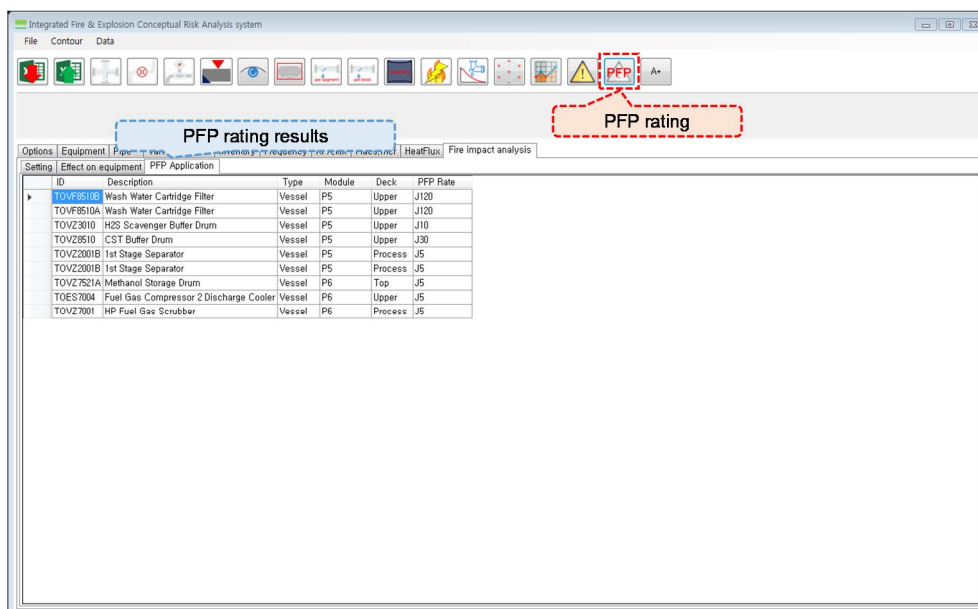


Fig. 58 PFP rating results by using IFECRA system

Table 22 Results of PFP rating by using CFD model (e.g. KFX)

ID	Descriptions	Type	Module		PFP rate
TOVF8510B	Wash Water Cartridge Filter	Vessel	P5	Upper	J120
TOVF8510A	Wash Water Cartridge Filter	Vessel	P5	Upper	J120
TOVZ3010	H2S Scavenger Buffer Drum	Vessel	P5	Upper	J10
TOVZ8510	CST Buffer Drum	Vessel	P5	Upper	J30
TOVZ2001B	1st Stage Separator	Vessel	P5	Process	J5
TOVZ2001B	1st Stage Separator	Vessel	P5	Process	J5
TOVZ7521A	Methanol Storage Drum	Vessel	P6	Top	J5
TOES7004	Fuel Gas Compressor 2 Discharge Cooler	Vessel	P6	Upper	J5
TOVZ7001	HP Fuel Gas Scrubber	Vessel	P6	Process	J5

Table 23 Results of PFP rating by using analytical model

(e.g. Phast)

ID	Descriptions	Type	Module		PFP rate
TOVZ7601	Cooling Water Expansion Drum	Vessel	P5	Top	J10
TOVF8510B	Wash Water Cartridge Filter	Vessel	P5	Upper	J120
TOVF8510A	Wash Water Cartridge Filter	Vessel	P5	Upper	J120
TOVZ3010	H2S Scavenger Buffer Drum	Vessel	P5	Upper	J10
TOVZ8510	CST Buffer Drum	Vessel	P5	Upper	J60
TOVZ2001A	1st Stage Separator	Vessel	P5	Process	J10
TOVZ2001A	1st Stage Separator	Vessel	P5	Process	J10
TOVZ2001B	1st Stage Separator	Vessel	P5	Process	J30
TOVZ2001B	1st Stage Separator	Vessel	P5	Process	J30
TOVZ7521A	Methanol Storage Drum	Vessel	P6	Top	J5
TOES7002	Fuel Gas Compressor 1 Suction Cooler	Vessel	P6	Upper	J5
TOES7003	Fuel Gas Compressor 2 Suction Cooler	Vessel	P6	Upper	J5
TOES7004	Fuel Gas Compressor 2 Discharge Cooler	Vessel	P6	Upper	J5
TOHE7001A	Fuel Gas Heater	Vessel	P6	Upper	J5
TOHE7001B	Fuel Gas Heater	Vessel	P6	Upper	J5
TOVF7001A	Fuel Gas Fine Filter	Vessel	P6	Upper	J5
TOVF7001B	Fuel Gas Fine Filter	Vessel	P6	Upper	J5
TOVF7525A	Subsea Methanol Injection Filter A	Vessel	P6	Process	J5
TOVF7525B	Subsea Methanol Injection Filter B	Vessel	P6	Process	J5
TOVZ7001	HP Fuel Gas Scrubber	Vessel	P6	Process	J5
TOVZ7002	LP Fuel Gas Scrubber	Vessel	P6	Process	J5
TOVZ7003	Fuel Gas Compressor 1 Suction Scrubber	Vessel	P6	Process	J10

TOVZ7004	Fuel Gas Compressor 2 Suction Scrubber	Vessel	P6	Process	J10
TOVZ2002	2nd Stage Separator	Vessel	S5	Upper	J5
TOVZ2002	2nd Stage Separator	Vessel	S5	Upper	J5
TOEP2501B	Stabilized Oil Cooler	Vessel	S5	Process	J5
TOEP2501A	Stabilized Oil Cooler	Vessel	S5	Process	J5
TOVZ7201	Hot Water Expansion Drum	Vessel	S6	Upper	J5
TOVF7526A	Methanol Supply Filter	Vessel	S6	Process	J5
TOVF7526B	Methanol Supply Filter	Vessel	S6	Process	J5
TOKA3101	LP1 Compressor	Vessel	S6	Process	J5

5. Conclusion

5.1. Summary

In pre-FEED stage, the process design is under development, therefore FRA input data are frequently changed and insufficient. In this time, the number of equipment is counted manually from the process design (e.g. PFD, P&ID). In addition, the process design does not provide a specific piping length. Hence, the process piping lengths are roughly estimated. For these reasons, the leak frequency calculation often obtains a large variance in the results. Furthermore, the lack of layout information and the process data, a 3D CFD fire simulation is not implemented in FRA because a 3D geometric model is not available.

Therefore, the main goal of this study is to develop an IFECRA system, which could be utilized to respond with the data quickly from the process design and to improve FRA results in pre-FEED stage. First of all, this study develops the IFECRA system to interface with the process simulator. Also, the process piping lengths are estimated using a routing algorithm to increase the accuracy of leak frequency calculation. In addition, the developed

IFECRA system is readily able to use a CFD model utilizing the simplified 3D model generation module. Finally, the IFECRA system can automate the calculation which is needed in FRA to increase efficiency. The developed IFECRA system displays the output from the graphical user interface (GUI).

From the case study, it is clearly demonstrated that the developed IFECRA system can improve the accuracy of risk analysis, because the IFECRA system is able to use the CFD model. First of all, a fire simulation result such as design effect zone is compared between CFD model and analytical model. In addition, the impact analysis and the rate of PFP are compared between CFD model and analytical model.

5.2. Findings

Through the case study, the findings of the study can be summarized. In order to apply the developed IFECRA system, a case study demonstrating a jet fire accident in the FPSO process area is performed. Through the observation of the case study, it is summarized that the risk analysis results used in the CFD model are more accurate than the analytical model. Consequently, it is

confirmed that the developed IFECRA system can increase the accuracy of FRA in pre-FEED stage.

6. References

- [1] Krueger, J. & Smith, D. 2003. A Practical Approach to Fire Hazard Analysis for Offshore Structures, *Journal of Hazardous Materials*, 104: 107–122.
- [2] FABIG 2009. Probabilistic Assessment of Fire Loads and Structural Response, FABIG Technical Note 11.
- [3] Paik, J. K. & Czujko, J. 2012. Engineering and design disciplines associated with management of hydrocarbon explosion and fire risks in offshore oil and gas facilities, *SNAME* 120: 1~39.
- [4] Paik, J. K., Czujko, J., Kim, B. J., Seo, J. K., Ryu, H. S., Ha, Y. C., Piotr, J. & Beata, M. 2011. Quantitative assessment of hydrocarbon explosion and fire risks in offshore installations, *Marine Structures* 24: 73~96.
- [5] Jin, Y. & Jang, B.-S. 2015. Probabilistic Fire Risk Analysis and Structural Safety Assessment of FPSO Topside Module, *Ocean Engineering* 104: 725~737.
- [6] Total 2008. Technological Risk Assessment Methodology GS EP SAF 041. Total.
- [7] DNV 2011. Leak Frequency Modeling for Offshore QRA Based on the Hydrocarbon Release Database. FABIG ISSUE 57.

- [8] OGP 2010. Process Release Frequencies, Risk Assessment Data Directory Report No.434-1. Oil and Gas Production.
- [9] Cox, A. W., Lees, F. P. & Ang, M. L. 1990. Classification of Hazardous Locations, UK: Institute of Chemical Engineers
- [10] NORSOK 2001. Risk and Emergency Preparedness Analysis NORSKO Standard Z-013. NORSKO, Oslo, Norway.
- [11] Kellogg, M. W. 1956. Design of Piping System, USA: A Wiley-Interscience Publication.
- [12] 김신형. 2014, 조선해양 CAD 환경에서의 선박 배관 자동배치 시스템 개발, *서울대학교 박사학위논문*.
- [13] KFX 2010. User's manual for Kameleon FireEx (2010). Computational Industry Technologies A/S, Stavanger, Norway.
- [14] Sávio, V. & Asmund, H. 2010. Fire CFD Modelling Applied to Offshore Design. Det Norske Veritas.
- [15] Jin, Y. & Jang, B.-S. 2015. Probabilistic Fire Risk Analysis and Structural Safety Assessment of FPSO Topside Module, *Ocean Engineering*, 104: 725~737.
- [16] Lee, K. S. Jang, B.-S. & Jin, Y. 2016. Study on Simplified Transient Fire Simulation Method in Fire Risk Analysis of Offshore

Process Area, *Proceeding of The Annual Autumn Conference (SNAK), Changwon, 3–4 November 2016.*

[17] Siegel. R. & Howell. J. R. 1992. Thermal Radiation Heat Transfer, USA: Hemisphere Publishing Corporation.

[18] DNV GL 2014. Phast Tutorial Manual, DNV GL, London, UK

[19] Total 2009. Layout GS EP SAF 021. Total

[20] Total 2009. Impacted Area, Restricted Area and Fire Zones GS EP SAF 253. Total.

[21] Dennis. M, 2001. Handbook of Fire and Explosion Protection Engineering Principles for Oil, Gas, Chemical and Related Facilities, USA: Elsevier.

7. Appendix

7.1. Appendix A: Example Rule Set of Process Piping Lengths

As detailed process piping arrangements are not available in pre-FEED stage, the estimation of piping length are made for each piping size within each isolatable segment. The following rule set which is presented in Fig. 59, is applied to roughly estimate the piping length between two equipment items, depending on the modules in which they are located.

	P4	P5	P6	P7	P8	S4	S5	S6	S7	S8	FD
P4	40.5	71.5	106.5	136.5	166.5	56.5	71.5	106.5	136.5	166.5	160.5
P5	71.5	40.5	71.5	106.5	136.5	71.5	56.5	71.5	106.5	136.5	130.5
P6	106.5	71.5	35.5	71.5	106.5	106.5	71.5	56.5	71.5	106.5	100.5
P7	136.5	106.5	71.5	40.5	71.5	136.5	106.5	71.5	56.5	71.5	70.5
P8	166.5	136.5	106.5	71.5	38.5	166.5	136.5	106.5	71.5	56.5	45.5
S4	56.5	71.5	106.5	136.5	166.5	40.5	71.5	106.5	136.5	166.5	160.5
S5	71.5	56.5	71.5	106.5	136.5	71.5	40.5	71.5	106.5	136.5	130.5
S6	106.5	71.5	56.5	71.5	106.5	106.5	71.5	35.5	71.5	106.5	100.5
S7	136.5	106.5	71.5	56.5	71.5	136.5	106.5	71.5	40.5	71.5	70.5
S8	166.5	136.5	106.5	71.5	56.5	166.5	136.5	106.5	71.5	34.5	45.5
FD	160.5	130.5	100.5	70.5	45.5	160.5	130.5	100.5	70.5	45.5	35.0

Fig. 59 Rule set of process piping lengths

For example, if equipment A and B are located in P5 then process piping length is 40.5m. If equipment A is located in P5 and B is located in P7 then process piping length is 106.5m

7.2. Appendix B: Constraint Conditions in Piping Algorithm

In this section demonstrates the constraint conditions in piping algorithm. The process piping algorithm such as rectilinear method is used for calculating the 6 piping nodes and piping lengths. In addition, the process piping algorithm such as A* method is used for generating 729 nodes between equipment. Total 8 constraint conditions are visually described from Table 24 to Table 31.

Table 24 Constraint condition 1

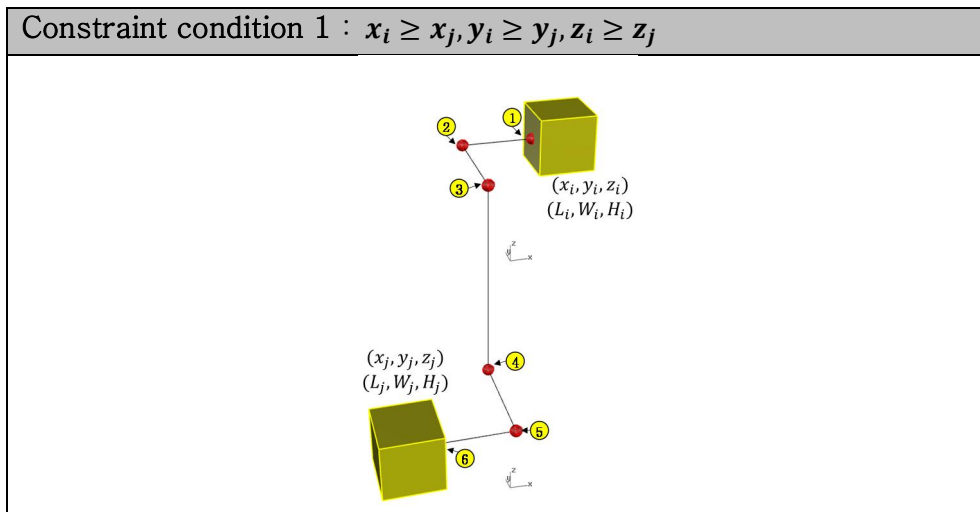


Table 25 Constraint condition 2

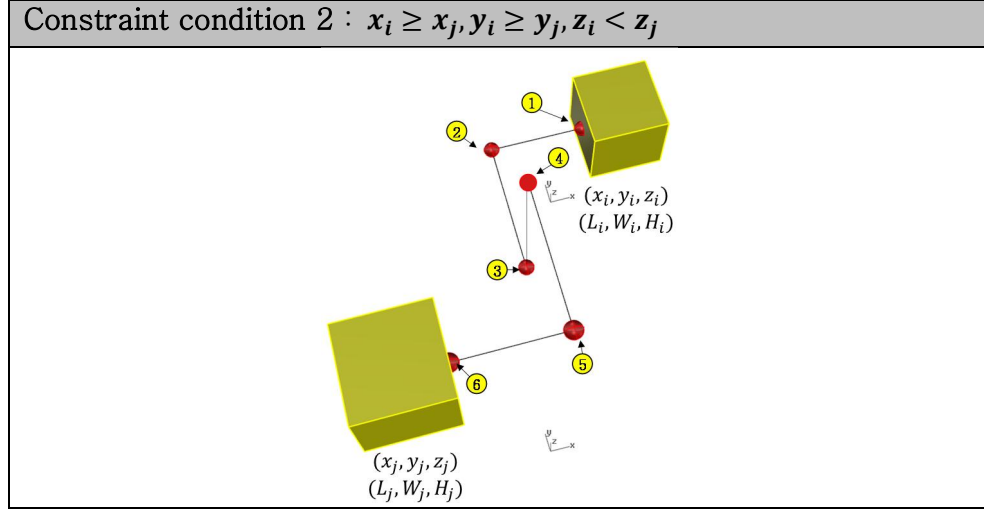


Table 26 Constraint condition 3

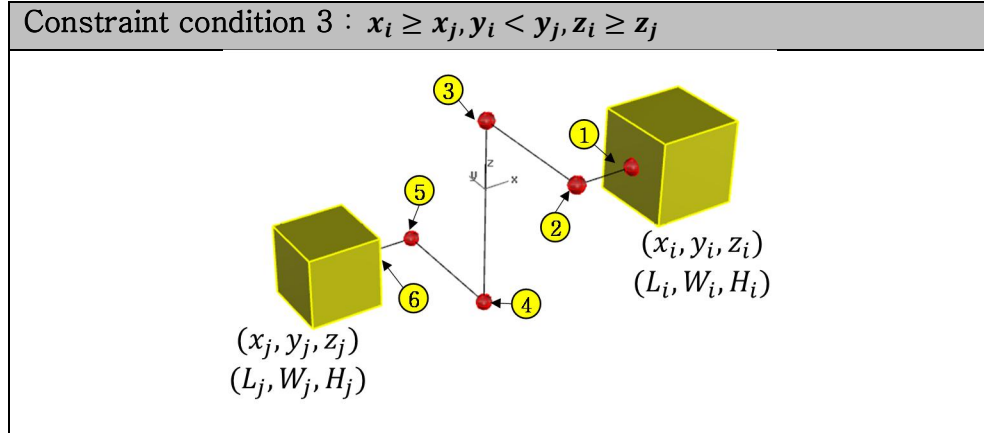


Table 27 Constraint condition 4

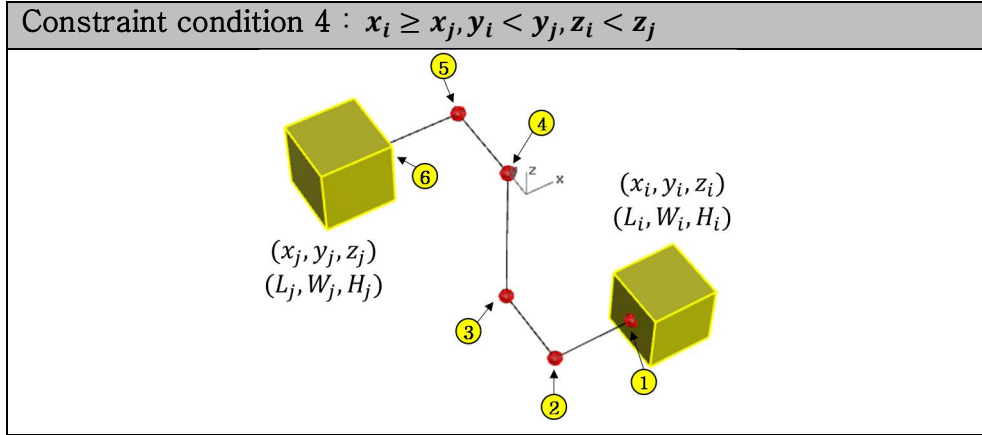


Table 28 Constraint condition 5

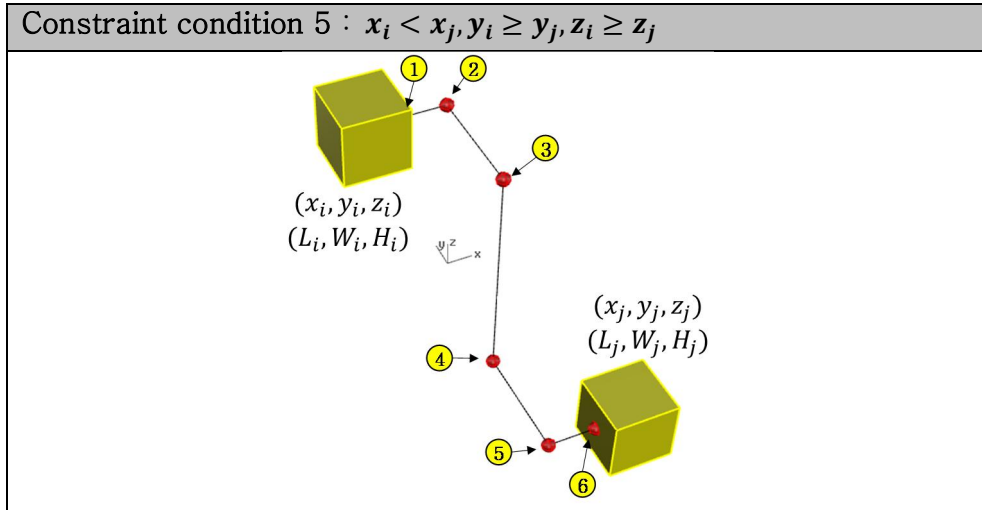


Table 29 Constraint condition 6

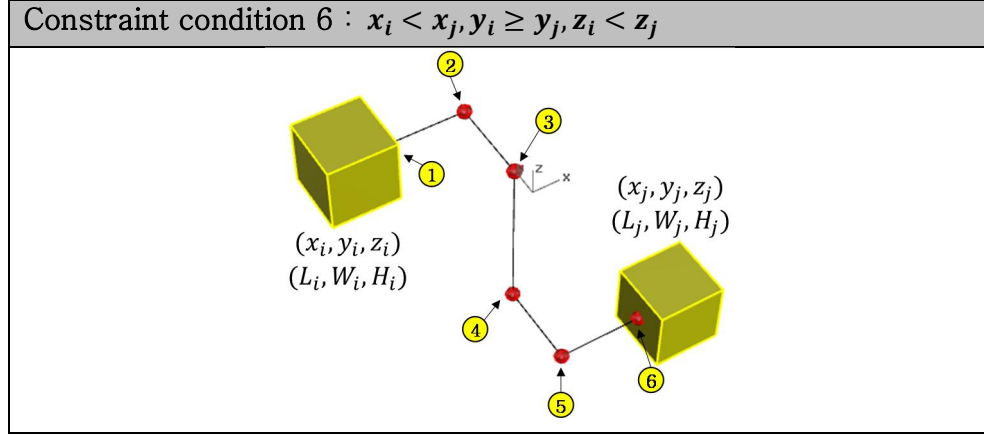


Table 30 Constraint condition 7

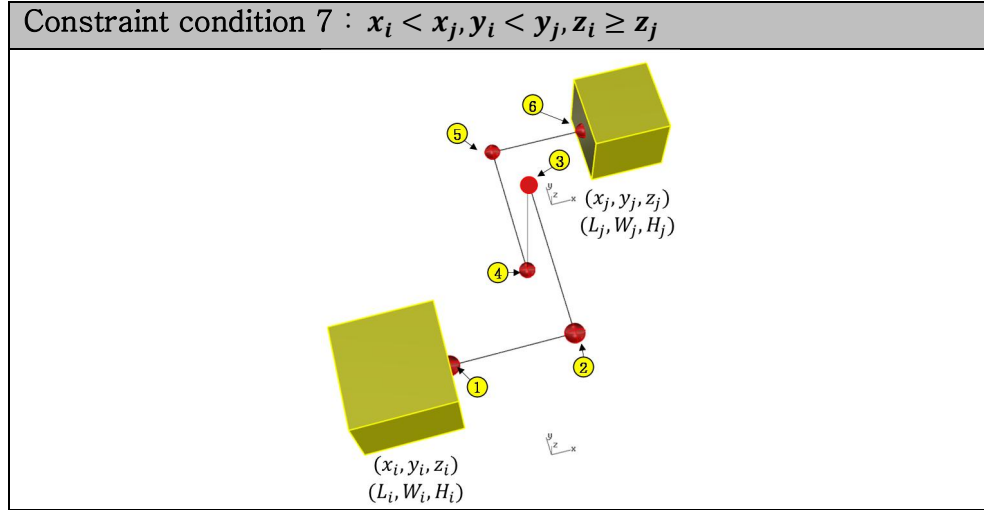
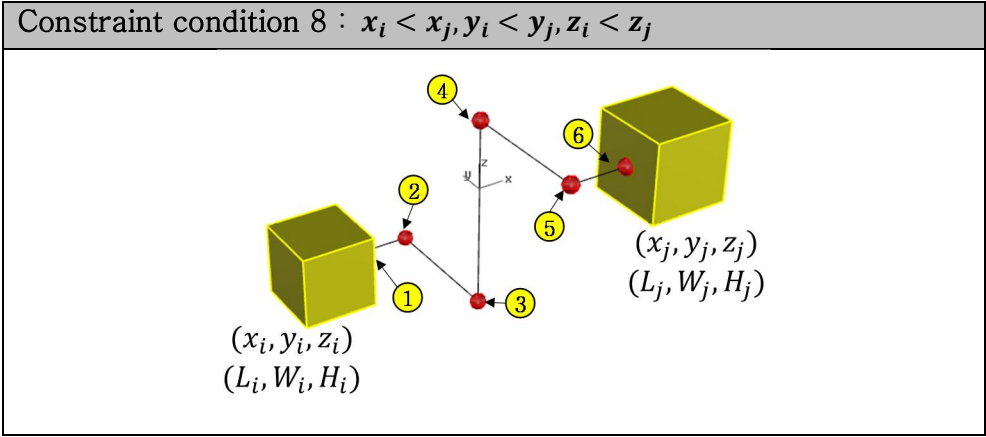


Table 31 Constraint condition 8



7.3. Appendix C: A Simple Example of A* Algorithm

A* method is a kind of searching algorithm that finds the smallest path cost from start to end. The heuristic equation of A* is given in below.

$$f(n) = g(n) + h(n) + W_{bending}$$

n	= The last node on the path
$f(n)$	= The minimum cost of all routes to the end node via node n
$g(n)$	= The cost of the path from the start node to n
$h(n)$	= The shortest path cost from node n to the end node
$W_{bending}$	= The bending cost

Fig. 60 presents visually for the cost of the path from the start node to n , $g(n)$, and the shortest path cost from node n to the end node, $h(n)$. In this study, $g(n)$ selects as 10 and $h(n)$ is a rectilinear distance such as below equation.

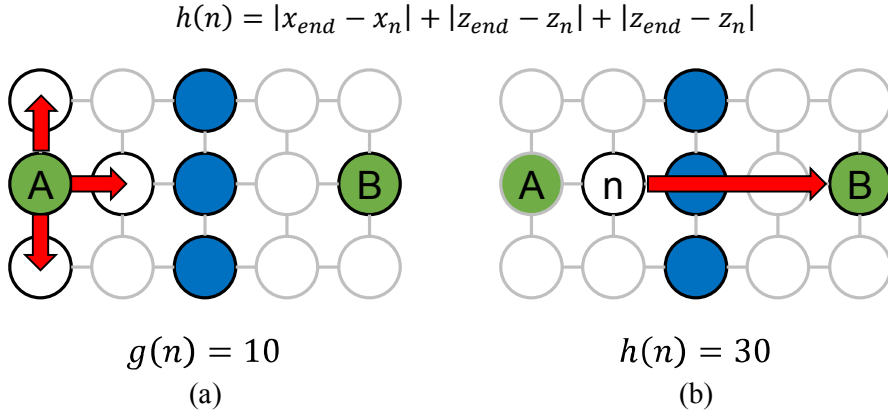


Fig. 60 Visual descriptions of (a) the cost of the path from the start node to n and (b) the shortest path cost from node n to the end node

In addition, path directions have set four direction without diagonal ways because there is no diagonal direction in the actual process piping in process area. Fig. 61 shows an example of path direction in this study. An example of path searching is visually described in Table 32.

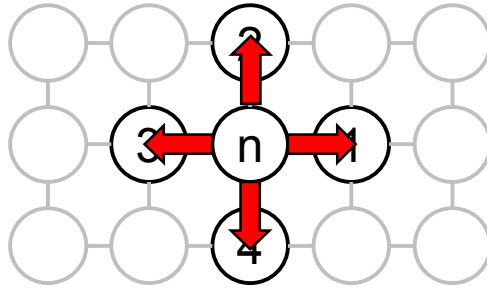
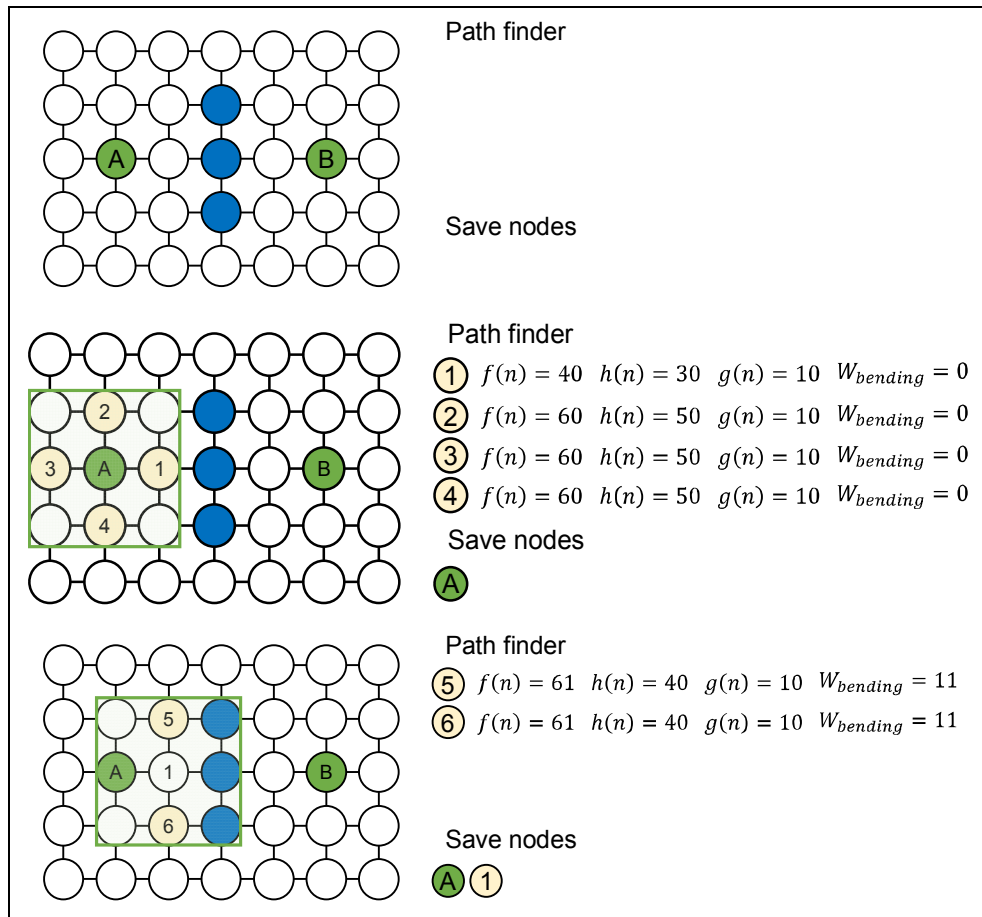
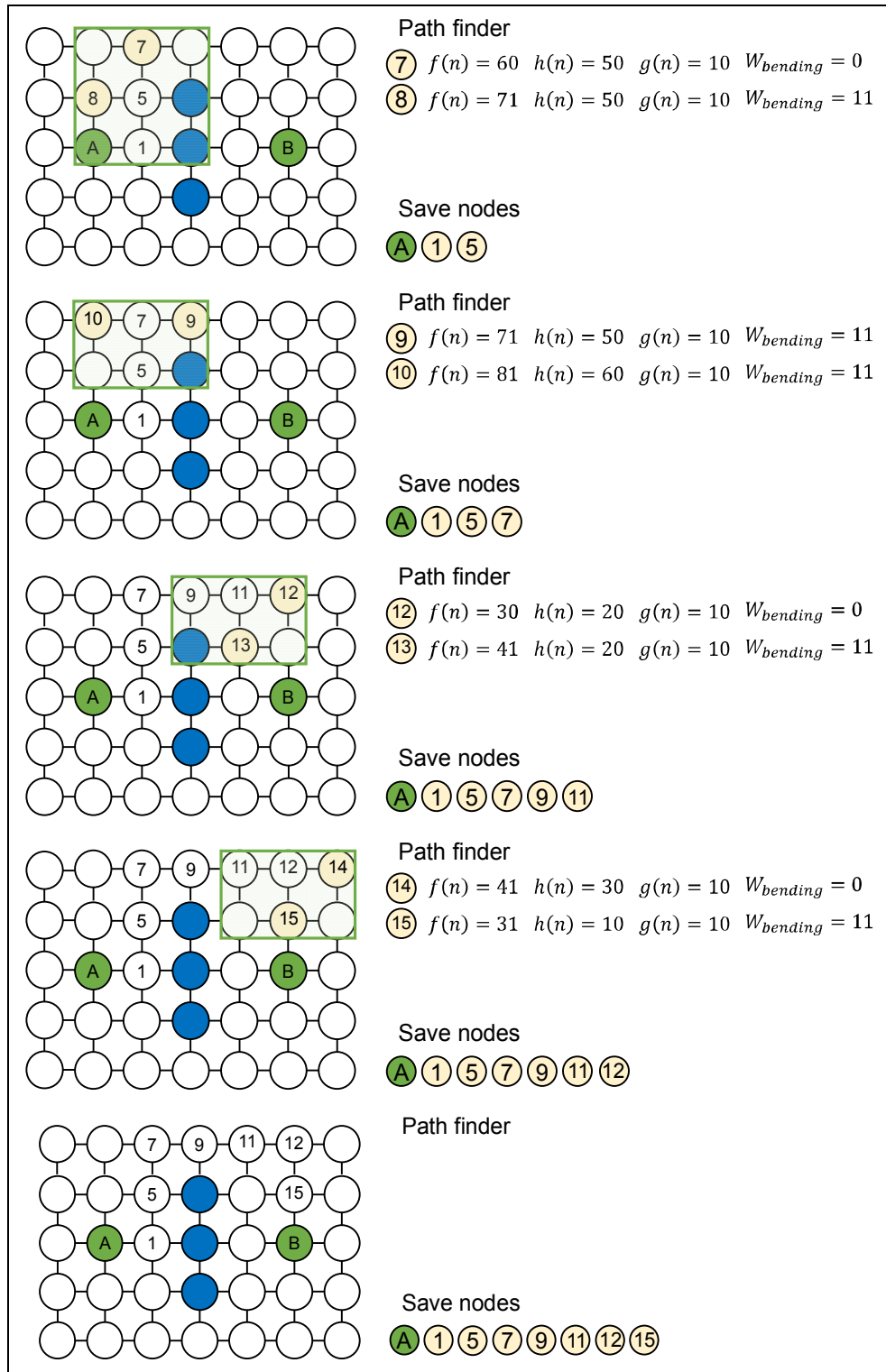


Fig. 61 Path directions from node n

Table 32 Simple example of path searching





초록

Pre-FEED 단계에서 개념적 화재 & 폭발 위험도 평가를 위한 기반 모델 개발

해양 플랜트는 가연성 오일과 가스를 정제하는 프로세스를 제한된 영역에서 가지고 있기 때문에 탄화수소 화재/폭발 사고가 발생할 가능성이 크다. 화재/폭발 사고는 전체 해양플랜트 위험도에 큰 비중을 차지하고 있기 때문에 최근 안전에 대한 선주의 요구사항이 점점 구체화하고 다양해지는 추세에 있으며, 설계에 소비되는 시간을 효율적으로 단축하기 위하여 빠르게 위험도를 판단할 수 있는 기술을 필요로 한다. 실제로 위험도 평가는 통상적으로 해양 프로젝트의 전체 설계 과정에 걸쳐 이루어지고 있으며, 각 설계 단계의 활용 가능한 정보와 데이터의 수준에 따라서 정성적인 평가로부터 정량적인 평가로, 간략한 해석으로부터 상세한 해석으로 평가 수준과 정확도를 높여 가면서 위험도 해석 결과를 설계에 반영하고 있다. 그렇지만 기존의 실제 프로젝트에서 수행되었던 초기 공정 설계 정보와 데이터 수준은 해양플랜트 상부구조의 화재/폭발 사고 위험도를 평가하는 데 있어서

유동적이지 못하다. 또한, 초기 공정 설계 정보와 초기 데이터 수준을 고려한 위험도 해석 결과는 보수적인 측면이 있다.

본 논문에서는 기존 방법들의 문제점을 극복하고자 Pre-FEED 단계에서 수시로 변하는 초기 공정 설계 값에 대응하고 해양플랜트 상부구조의 화재 위험도 평가 방법을 개발하기 위하여 기존 방법을 조사 및 분석하였다. 기존 방법에 대한 조사 및 분석 결과를 바탕으로 위험도 평가에 필요한 모든 계산과 데이터 전달을 체계적으로 관리할 수 있는 통합 시스템 즉, Integrated Fire & Explosion Conceptual Risk Analysis system (IFECRA)을 확립하였다.

화재/폭발 위험도 평가에 필요한 공정 데이터와 레이아웃 데이터를 정의하였다. 공정 시뮬레이터에서 추출한 데이터를 전달하는 표준 data transfer sheet 을 확립하였고, IFECRA 시스템에서 표준 data transfer sheet 을 import 할 수 있는 모듈을 개발 완료 하였다. 초기 공정 데이터를 가공하여 IFECRA 시스템 내 누출 빈도수 계산을 자동으로 계산하는 모듈을 개발 완료 하였고, 화재/폭발 해석에 필요한 3D model 자동 생성 모듈을 개발 완료하여 화재/폭발 시뮬레이터와 연동할 수 있도록 하였다. 3D model 자동 생성 모듈로부터 생성된 모델을 이용하여 3D CFD 시뮬레이션을 수행할 가능성을 제공한다. 기존 2D simplified 화재/폭발 시뮬레이션 결과보다 상대적으로 정확도 높은 결과를 설계에 반영함으로써 설계비용 감소와 설계지연을 단축할 가능성을 제공한다. 위험성 평가 모듈은 시스템 내부 누출빈도 수와

점화확률 계산 결과와 화재 시뮬레이터로부터 계산된 결과값을 입력 받아 평가에 필요한 Accidental Design Load (DAL) 값을 계산하여, 화재 위험도 평가를 가능하도록 하였다. 본 논문에서 개발한 IFECRA 시스템을 활용하여 확률론적 화재 위험도 평가 방법에 필요한 데이터를 자동으로 계산하였고, CFD 모델과 해석적 모델 화재 시뮬레이션 결과를 이용하여 설계 effect zone 를 계산하였다. 계산된 설계 effect zone 을 이용하여 프로세스 장비의 파손여부와 파손된 장비의 PFP rate 결정을 서로 비교하였다.

화재 위험도 해석 결과 본 논문에서 제시하는 IFECRA 시스템을 활용하여 수행한 위험도 해석 결과가 기존 방법보다 상대적으로 정확함을 확인하였다.

주요어 : Quantitative risk assessment, Fire risk analysis, Offshore, Topside, Process area, Integrated system, Computational fluid dynamics, Analytical model

학 번 : 2015-21169